91602
Form 82-10

COMMERCIAL COPY
Please Credit Ontario Hydro Research If
Reproduced in Whole or in Part

LEGAL NOTICE

This report was prepared by Ontario Hydro and, while effort has been made to assure the accuracy and applicability of the material contained herein, neither Ontario Hydro nor any person acting on its behalf:

(a) makes any warranty, express or implied with respect to the use of any information, apparatus, method or process disclosed in this report or that such use may not infringe privately owned rights; or

(b) assumes any liabilities with respect to the use of, or for damages resulting from the use of, any information, apparatus, method or process disclosed in this report.

ontario hydro
research division

HEADGATE ROLLER PATH REPAIR: A FEASIBILITY STUDY OF THE WELDING OPTION

Report No. 90-337-K
T.W. Lau
and
M. Mathers
Metallurgy Section
Metallurgical Research Department

ABSTRACT

The feasibility of applying welding technology to repair headgate roller path plates was studied. The welding option was considered due to the attractive economic aspects. This study involved the development of the repair procedure which included material and process selection, with optimization of gouging, welding and grinding parameters. A first mock-up was done to allow the estimation of stress levels and the design of a distortion control system. The second mock-up tested the distortion control system selected, recorded the temperatures on the plate and in the concrete, monitored distortion, and measured the load on the plate.

It was found that distortion could not be eliminated completely by the distortion control system. The residual stress levels in the plate were very high, up to the yield stress levels of the deposited material and the base plate. There are uncertainties about how the residual stresses will be redistributed after the plate had been loaded by the passage of the wheels. Hence, the welding option is not recommended at this time. It is also suggested that the welding option warrants further development, particularly for applications where limited localized repairs are necessary.

ntis	file	date	report no.
81-205-581	823.124	February 8, 1991	90-337-K

91602
new 82-10

92-00885/

ontario hydro
research division

EXECUTIVE SUMMARY

HEADGATE ROLLER PATH REPAIR: A FEASIBILITY STUDY OF THE WELDING OPTION

T.W. Lau and M. Mathers

The feasibility of applying welding technology to repair headgate roller path plates was studied. The welding option was considered due to the attractive economic aspects. As discussions of the weld repair option progressed from conception, the possibility of jeopardizing the dam through distortion and structural damage was considered. These concerns made the weld repair option conditional upon results obtained from full scale mockups and simulations of this approach. The first mock up was built to allow the estimation of stress levels and the design of a distortion control system. The second mock-up tested the distortion control system selected, recorded the temperatures on the plate and in the concrete, monitored distortion, and measured the load on the plate.

This feasibility study has provided valuable information on the welding option for headgate roller plate repair. The following conclusions were drawn:

1. The gouging procedure developed provided proper surface preparation for the subsequent welding build up. The welding procedure gave an excellent rebuilt surface with good surface profile and penetration.

2. The first mock-up provided information for the estimation of stress levels and the design of a distortion control system. The calculated stress was verified by the measurements made in the second mock-up.

3. The distortion control system in the second mock-up did not eliminate distortion completely. However, the distortion observed was small. There were residual stresses, up to the yield stress level, present in the plate.

4. There were observations suggesting distortion of the I-beam. The amount, if any, was small and within the limit of experimental errors of the measuring technique used.

job	file	date	report no.
81-205-581	823.124	February 8, 1991	90-337-K

5. Due to the distortion observed, high levels of residual stresses, and the uncertainty in the possible redistribution of the stress, the welding option for roller plate repair is not recommended at this time.

6. The welding technology for repair warrants further development. However, future development should be focused on applications in localized limited repair.

TABLE OF CONTENTS

		Page
1.0	INTRODUCTION	1
2.0	OBJECTIVES	2
3.0	EXPERIMENTS AND RESULTS	3
3.1	Filler Wire Selection and Repair Procedure Development	3
3.1.1	Filler Wire	3
3.1.2	Gouging Procedure	4
3.1.3	Welding Procedure	5
3.1.4	Grinding Procedure	6
3.2	The First Mock-Up	6
3.2.1	Gouging and Welding Results	7
3.2.2	Distortion Results	7
3.3	Restraint System and Stress Estimation	8
3.3.1	Proposed Restraint Systems	8
3.3.2	Stress Estimation of The Selected Restraint System	9
3.4	The Second Mock-Up	9
3.4.1	Gouging, Welding and Grinding	10
3.4.2	Temperature Measurements	10
3.4.3	Distortion	11
3.4.4	Stresses in The Mock-Up	12
3.4.5	Repair Time Requirement	13
4.0	DISCUSSION AND RECOMMENDATIONS	14
5.0	CONCLUSIONS	16
ACKNOWLEDGEMENTS		17
TABLES		18

TABLE OF CONTENTS

	Page
FIGURES	27
APPENDIXES	
Appendix A	46
Appendix B	57
Appendix C	65
Appendix D	75
DISTRIBUTION	last page

LIST OF TABLES

		Page
Table 1	Composition of Stoody 110-0	18
Table 2	Recommended Gouging Parameters	18
Table 3	Recommended Parameters for Welding Operation	19
Table 4	Gouging Parameters Used for The First Mockup	20
Table 5	Parameters Used for Welding of the First Mockup	21
Table 6	Distortion of the First Mockup	22
Table 7	Distortion of the Second Mockup	23
Table 8	Distortion of the Second Mockup After Removal of The Restraint System	24
Table 9	Selected Load Cell Readings From Appendix D	25
Table 10	Residual Stresses of Mockup #2	26

LIST OF FIGURES

		Page
Figure 1	Pictorial View of Roller Path	27
Figure 2	Mechanized Gouging/Welding System	28
Figure 3	As Gouged Profiles	29
Figure 4	A Bead Profile	30
Figure 5	Distortion Measurement Points on Roller Path Mockup #1 All Dimensions in Millimetres	31
Figure 6	As Gouged Surface Appearance	32
Figure 7	As Welded Surface Appearance	33
Figure 8	Proposed Distortion Control For Roller Path Weld Repair Using Anchor Bolts	34
Figure 9	Proposed Distortion Control For Roller Path Weld Repair Using Gouged and Welded Rivet Heads	35
Figure 10	Proposed Distortion Control For Roller Path Weld Repair Using Temporary Structural Stiffening Members	36
Figure 11	Proposed Distortion Control For Roller Path Weld Repair Using Jack Post Support From Stop Log Wall	37
Figure 12	Proposed Distortion Control For Roller Path Weld Repair Using Load Transferring Side Plates	38
Figure 13	Conceptual Diagram of Mockup #2	39
Figure 14	a) Profile of Roller Track Plate After Gouging	40
Figure 14	b) As Gouged Surface	40
Figure 15	As Welded Surface	41
Figure 16	As Ground Surface (Manually Ground)	41

LIST OF FIGURES

		Page
Figure 17	Locations of Thermocouples	42
Figure 18	Distortion Measurement Locations on Roller Path Mockup #2	43
Figure 19	Probable Distortion of the I-Beam	44
Figure 20	Abitibi Canyon-Head Gate Track Repair Simulation Locations of Residual Stress Measurement Rosettes	45

91601
new 82-10

ontario hydro
research division

TO Mr. A.M. Wilson
Manager
Hydraulic Stations Dept
N10-B06

HEADGATE ROLLER PATH REPAIR: A FEASIBILITY STUDY OF THE WELDING OPTION

T.W. Lau and M. Mathers

1.0 INTRODUCTION

At many hydraulic generating stations, the headgates cannot be properly closed due to damage on the roller path plates. Some of these roller path plates were fabricated in semi-killed, grade UNS G10150 hot rolled plain carbon steel meeting requirements of ASTM specification A830. This material has a relatively low yield strength of about 26 ksi. Premature deterioration of the roller path plates resulted from a combination of marine growth, pitting corrosion, and wear due to the passage of the headgate wheels. About 165 headgates need to be repaired. Hence, any repair technique which can minimize the cost will represent substantial saving for Ontario Hydro.

Several repair techniques were considered by the Hydraulic Generation Operation Division. These include replacing the plate, placing a new plate on top of the existing one, and rebuilding the existing plate by welding. The welding option, using the Pulsed Gas Metal Arc (P-GMA) process, was investigated by the Research Division and the findings are being reported in this document. Localized heating due to operations such as welding will introduce residual stress or distortion to the plate. The stress in the plate will eventually be transferred to the concrete supporting the plate. Whether the additional stress can be safely carried by the concrete dam structure was not known. A feasibility study, therefore, was required to assess the extent of the residual stress and/or distortion. This study can be easily justified since the welding approach does have attractive aspects such as simplicity and economics. The welding approach does not require substantial adjustment of the headgate itself, and the estimated cost is about half that of the other options.

The Abitibi Canyon GS was scheduled for outage in September 1990, and could be the first headgate to be repaired. At Abitibi Canyon GS, the roller path plate measures 10 m high, 444 mm wide, and 35 mm thick. A relatively uniform groove of about 6 mm (1/4 in.) has been removed by the wheel. The groove is about 150 mm wide. In addition, there are deeper pits

scattered over the grooved area. The damage at Abitibi Canyon GS represents one of the worst cases. Structurally, the plate is held in place by rivetting into an I-beam which is embedded in a layer of secondary concrete. Figure 1 gives a pictorial view of the headgate roller plate. Note that a side plate is connected to one side of the roller path plate, and any distortion of the roller path plate may cause movement of the side plate.

This report summarizes the results obtained in the welding option feasibility study, using mechanized P-GMAW, launched in March, 1990. The mechanized approach was studied due to its high efficiency and the fact that this particular application can be effectively handled by mechanized welding. The study was carried out under the assumption that the repair technique developed would be applied at Abitibi. During the course of the project, it was found necessary to have a better surface finish than available by manual grinding. The portable compact robot developed at Ontario Hydro Research Division (OHRD) for hydraulic turbine runner repair was then briefly studied as an instrument for providing an acceptable surface finish.

2.0 OBJECTIVES

The primary objective of the project was to evaluate whether welding technology can be used in repairing the roller path plates. However, it was necessary to develop a repair procedure first. The repair procedure includes the following operations:

1) Surface preparation using plasma arc gouging to generate a smooth profile and a clean surface for weld metal deposition.

2) Weld metal deposition to build up the plate.

3) Grinding to refinish the surface to the original plate profile.

In developing the repair procedure the following issues were addressed:

- filler wire (composition, brand, diameter) and shielding gas selection
- optimum gouging, welding, and grinding parameters
- options of welding power source and other mechanical apparatus
- distortion effects and prevention methods

The criteria to judge the acceptability of the technology are as follows:

- weld deposition and surface finish qualities
- the magnitude of distortion and the residual stress level
- the cost and time requirement of the repair

This project studied the issues and evaluated the welding repair option according to these criteria.

3.0 EXPERIMENTS AND RESULTS

The experimental part of the project was divided into the following tasks:

1) Filler wire and shielding gas selection and repair procedure development.
2) A first mock-up to study the extent of distortion.
3) Stress level estimation and restraint system design based on the results of the first mock-up.
4) Fully instrumented second mock-up.

3.1 FILLER WIRE SELECTION AND REPAIR PROCEDURE DEVELOPMENT

A mechanical P-GMAW welding system was targeted for Abitibi Canyon, as already mentioned. The mechanical welding system consisted of a Gullco P-KAT carriage (#GK-191-P36A) for vertical movement and a BUG-O 5300 OSCILLATOR for horizontal weaving. The P-KAT carriage was modified by the addition of a circuit to accept a stop/start signal. Thus, during the horizontal traverse the P-KAT carriage would be stationary, and at the end of the traverse, the carriage would move upward (welding) or downward (gouging) for a given distance. This incremental distance depended on the P-KAT carriage speed setting and the dwell time. The assembled system with a gouging head is shown in Figure 2. A power source and its accessories (a Miller Intellipulse 650 power supply) were shipped from Timmins District to the Research Division for the welding procedure development work. A Binzel MB501 water cooled torch was used. The gouging used an L-TEC PCM 100 plasma gouging console with appropriate torches (L-TEC PT-17-A and PT-17-AM). Most of the grinding was done manually, using the P-KAT carriage to raise or lower a modified air grinder. This was accomplished through a lever control on the grinder, and a dedicated circuit to control the travel of the P-KAT carriage.

Based on the above set-up, a proper filler wire was selected and a repair procedure was developed.

3.1.1 Filler Wire

The properties requirements of the deposited material, which would become the load bearing part of the roller path plate, depended primarily on the filler wire chosen. The filler wire requirements were reviewed by M.J. Tinkler. The relevant document is attached as Appendix A. In summary, the filler material must have sufficient yield strength to withstand the load from the passage of the wheels, adequate wear resistance, reasonable corrosion resistance in an aqueous environment, good resistance to marine growth, low as deposited hydrogen and good compatibility to the 1015 base plate. Based on the above requirements, Stoody 110-0 filler wire was recommended by Dr. G. Bellamy. The composition of the wire, as supplied by Stoody Engineering, is listed in Table 1.

The deposit from this wire was quite fluid, and this dictated that the weld beads be deposited

horizontally, starting from the lower end of the roller plate. The fluid weld pool also required the welding arc to be extinguished at the end of each weld bead for a short period , to allow the weld metal to solidify before the next bead was deposited. This was accomplished through a relay circuit triggered by the BUG-O weaver, turning the welding machine's wire feeder trigger on and off.

3.1.2 Gouging Procedure

The purpose of gouging was to prepare a relatively uniform and smooth starting surface profile for weld bead deposition. A smooth starting surface profile led to a less rough built-up surface. Also, the gouged depth could be made to be a close multiple of the bead height to minimize the amount of grinding to be done after welding. The bead height was set once the welding parameters were chosen.

Gouging was done in the horizontal position (2G) with downward progression. This procedure allowed gravity to aid the removal of the molten metal. The gouging parameters recommended are listed in Table 2. Using this set of parameters, the average gouged depth per pass depended on the weaving speed and P-KAT carriage settings (speed and dwell time). Using a weaving speed of 26.4 mm/s, a KAT speed of 8.3 mm/s and a dwell time of 1/8 s, the average gouged depth was about 4 mm. When dealing with the larger plate in the field, it is expected that the gouged depth using the same parameters will lead to a shallower depth, due to the larger heat sink effect of the larger plate. A greater gouged depth can be obtained by slowing down the weaving speed. The adjustment of weaving speed in the field can be easily done with no adverse effects.

Figure 3a shows the transverse cross-section gouged profile preferred for an anticipated two layer build-up. Such a profile can be generated by two or more gouge passes. The first gouge pass should use a relatively slow weaving speed to generate the steep, deeper central groove. The second and subsequent passes should cover a wider area and use a faster weaving speed, to generate the shallower outer profile. The deeper central region was made in anticipation of deeper cavities lying within the general groove on the roller path plate in Abitibi Canyon GS. The central deeper region would be filled by the first weld deposit layer. The shallow grade (about 20 to 30) at the extremities of the profile ensured proper fusion between the weld bead and the base metal at the edges of the repaired area.

The gouged depth varied over the length of the simulated roller path plate (ranging from 3 to 5mm). A longitudinal cross-section of a gouged profile is shown in Figure 3b. The gouged depth variation was due to at least two reasons. In the starting region, the gouged depth increased gradually until an equilibrium value was reached. This was a built in variation of the gouging process, due to the overlapping of adjacent grooves. If the material removal rate was constant, the second traverse would produce a deeper groove than the first traverse since some material had already been removed by the first traverse. However, the deeper groove also increased slightly the arc length, reducing the material removal rate. The apparent equilibrium depth was reached when the material removal rate was reduced to a level which no longer could

increase the depth of the groove. The arc length was not constant over the entire length of the plate due to the difficulty in aligning the P-KAT carriage track with the roller path plate. This resulted in an arbitrary depth variation depending on the alignment. However, these variations in depth were acceptable and posed no significant problems.

It was mentioned that different gouging torches were used for the first (PT-17-A) and second (PT-17-AM) mock-ups. This had no significant effects on the results obtained. Gouging was a relatively fast operation, and it took about 35 min. to gouge a patch 127 mm wide and 2000 mm long. The peak temperature reached at the back of the roller path plate was 222 C, and 166 C in the concrete in the second mock-up. After gouging, the gouged area was covered by a thin layer of oxide. It is recommended that proper cleaning using a grinder be done to avoid possible lack of fusion defects in welding.

3.1.3 Welding Procedure

Since the filler material generated a relatively fluid weld pool, the only practical welding position was the horizontal position with an upward progression. Thus the previous bead acted as a ridge support for the weld pool. The weld pool fluidity also limited the usable heat input. Consequently proper interbead fusion and penetration into the base metal rely on correct interbead spacing and the torch angle, rather than high heat input. The use of lower heat input was also desirable from the distortion perspective. The interbead spacing also significantly influenced the as deposited surface roughness. A proper interbead spacing minimized the amount of grinding required.

Table 3 lists the typical welding parameters used. To lay the first weld bead, the torch angle was set almost perpendicular to the roller path plate to build up a ridge. Subsequently, the torch angle was set at 15 to the horizontal, pointing at the toe of the previous bead. At the current and voltage settings shown in Table 3, the wire feed speed was at the lower limit of the allowable range. Thus the wire melting rate and the deposition rate was lower than normal. This was done to avoid excessive crown build up from molten filler material and to allow the weld pool to penetrate into the base metal. The interbead spacing was determined by the P-KAT carriage speed setting and the dwell time. Thus at a P-KAT carriage speed of 2.2 mm/s and a dwell time of 3.2 s, the interbead spacing would be about 5.2 mm, after accounting for the time required for the P-KAT carriage to reach the set speed.

If for any reason, welding had to be stopped, slag removal and cleaning by grinding of the previous bead and the general area were necessary before re-starting the arc. The interbead spacing should also be reduced by about 20%. This was done by manually moving the welding head. These actions avoided fusion defects at the stop/start area. As in any welding, a definite dwell time at the start and the end of a bead was necessary to avoid defects in those areas. As a result, the bead profile, seen from a transverse cross-section of the roller path plate, would be similar to that shown in Figure 4. If a second layer of weld beads were to be placed, the humps at the extremities of the first weld bead (represented by shaded areas in Figure 4) had to be removed by grinding to prevent fusion defects at the intersections among the first, second layers

of weld metal and the base plate. Prior to the deposition of a second layer of weld metal, grinding of the first layer weld metal to remove slag and surface oxide, as in general surface preparation for welding, is required.

As in gouging, the difficulty in aligning the P-KAT carriage track with the plate led to a variation of the deposit height over the length of the roller path plate. This variation could be managed by the grinding process, but this meant that the weld deposit height must be at least 2 mm higher than the roller plate surface.

3.1.4 Grinding Procedure

A limited amount of work in grinding was done. The BUG-O weaver was unable to tolerate the load associated with grinding. Hence, manual grinding was planned for use at Abitibi Canyon. As already mentioned, the P-KAT carriage was used to partly support and move the air grinder. However, it became obvious that manual grinding was not capable of obtaining the required surface finish. The OHRD compact robot showed the capability to achieve an acceptable finish, if used to do the final fine grinding. Currently, the compact robot uses only a force sensor for guiding the robot during grinding, and therefore, follows the general profile of the weld deposit. Some modification in the control software is needed to achieve the required profile.

3.2 THE FIRST MOCK-UP

The purpose of the first mock-up was to study the extent of the distortion and to use the information to design a distortion prevention system. The mock-up consisted of a simulated roller path plate stitch welded to an I-beam. A side plate was also stitch welded to the roller path plate. The schematic diagram and the dimensions of the mock-up are shown in Figure 5. It should be noted that the simulated plate was machined out of a different material (516 G70). The UNS G10150 material used in Abitibi Canyon GS was not readily available. Since the 516 G70 steel has a higher yield strength, the stresses generated by the welding operation in the mock-up would be higher than the actual stresses expected in the actual situation. Also the I-beam used (203 mm), was a smaller size than the actual one at Abitibi Canyon GS (381 mm).

To monitor distortion caused by the gouging and welding operations, a reference frame was set up behind the roller path plate. The perpendicular distances between sets of two points, with one lying on the reference plane and the other on the roller path plate plane, were monitored. Any change in the distance between the two points in a set would indicate movement of the roller path plate through distortion. The locations of these point sets are also shown in Figure 5. Measurements of the distances between these point sets were taken both after gouging and welding.

3.2.1 Gouging and Welding Results

Table 4 lists the gouging parameters used for the 2 gouging passes of the first mock-up. These parameters were very similar to the recommended parameters, which were the results of revision after the experiments. The first gouging pass removed about 4 mm of material from a width of 65 mm in the centre line region of the plate. The second pass spanned a width of 117 mm. The depth of the central region increased to about 8 mm, while the outside regions had a maximum depth of about 5 mm. Figure 6 shows the appearance of the as gouged surface. Table 5 lists the welding parameters used in the first mock-up. Figure 7 shows the welded surface after the two welding passes. It can be seen from Figure 7 that the bead spacing, heat input etc. were not optimized. There was a slight weld pool rolling problem. These problems were corrected, resulting in the recommended parameters listed in Table 3.

3.2.2 Distortion Results

Table 6 summarizes the distortion measurements made. Level 1 was at the top of the plate and Level 5 was at the bottom of the plate. Location A was at the left side of the plate (the far side from the side plate) and Location D was at the right side of the plate (adjacent to the side plate). Location H was at the back flange of the I-beam. Finally, points 6E, 6F, and 6G were used to monitor the movement of the side plate (See figure 5). Plumb lines and a straight edge were used to make the measurements. This measuring technique might be accurate to within 1 mm. This level of accuracy was considered to be sufficient since it was decided that any distortion lower than the detectable level would be acceptable.

The numbers in Table 6 are the changes in distances of the point sets after an operation. Since the reference was at the back of the roller path plate, the positive values in distance changes suggested the general forward curving of the plate upon the vertical and horizontal axis (see Figure 5). However, local movements were complex. The forward curving movement of the plate was not symmetrical upon the vertical axis. The right side of the roller path plate distorted more. This may be related to the fact that the roller path plate was not centred upon the I-beam, but off to the left. Using the horizontal centreline as a reference, the central region of the plate moved forward significantly more than the top or bottom regions. There is no apparent reason for this phenomenon, except that this may be related to the stop/start positions during welding. The inward movement of the side-plate was due to the forward curving of the roller path plate. The different levels of movement measured at 6E, 6F and 6G were due to the different distances of the points from the centre of rotation.

The mock-up showed that distortion was a serious problem. The distortion, of course, was due to the localized heating by the gouging and welding operations, and the subsequent expansion and contraction of the weld metal and the base plate. The observed degree of distortion showed that it was not possible to eliminate or minimize distortion to a tolerable level by changes in the gouging or welding parameters. However, changes that would affect the heat flow pattern, such as changes in the sequence of weld bead deposition, would at least change the way which the plate would be distorted. Restraint systems were designed to control the distortion. Prevention

of distortion also meant that there would be residual stress in the roller plate and the restraint system, and judging from the distortion, the stress in the restraint system and therefore the surrounding concrete, would be tensional. It was necessary to know the magnitudes of the stresses, to ensure that they did not exceed the relatively low tensile strength of concrete. The measurements made in this mock-up were used to estimate the magnitude of the residual stresses in the roller path plate, and hence the peak stresses imposed on the dam's structure.

3.3 RESTRAINT SYSTEM AND STRESS ESTIMATION

The aim of using a restraint system was to prevent distortion in the roller path plate and to transfer the consequent tensile stresses to the concrete surrounding the restraint system. It is important that the chosen restraint system would distribute the stresses in such a way that there would be no excessive stress on any part of the concrete dam. At the same time, the restraint structure should be simple to build but strong enough to prevent or minimize distortion of the roller plate.

3.3.1 Proposed Restraint Systems

Several approaches to prevent distortion were proposed for consideration by the Civil Department. These concepts are shown in Figures 8 through 12. Figure 8 shows the distortion control concept using anchor bolts. A column of anchor bolts, on each side of the would be weld repaired region, were to be placed into the secondary concrete before the gouging and welding operations. The size and the spacing of the anchor bolts would depend on the expected stress magnitude. This approach was rejected because putting stresses in the secondary concrete was seen as undesirable. Figure 9 shows the approach through gouged and welded rivet heads. This approach aimed only to reinforce the rivet heads, and would be used if the distortion seen on the first mock-up was deemed to be acceptable.

Figures 10 and 11 illustrate concepts using temporary restraint systems. Figure 10 shows the approach using temporary structural stiffening members, and Figure 11 shows the control concept through the use of jack post support from the stop log wall. The use of a temporary structure implies that some springback would occur unless some form of stress relief process such as post weld heat treatment or peening was done before removal of the restraint system. Obviously, any form of post weld heat treatment is not practical. It is difficult to estimate how much stress relief can be obtained through peening. Subsequently, the amount of springback cannot be predicted. It was also decided that any amount of springback upon removal of the restraint system would be unacceptable.

Figure 12 shows the distortion control system using an added restraint plate to transfer the stress to the primary concrete and angle brackets to anchor the side plate. Anchor bolts would be used to secure the restraint plate onto the primary concrete. This system is relatively simple and was tentatively accepted by staff at the Civil Department. The size and frequency of the bolts and angle brackets required were calculated through a stress estimation done by staff of the

Mechanical Research Department. The data available from the first mock-up was used as the basis of the stress estimation. The results are shown in the following section.

3.3.2 Stress Estimation of the Selected Restraint System

Precise prediction of the magnitudes and distribution of stresses generated by welding is very difficult, if not impossible, even using currently available finite element analysis techniques. This is due to the complication introduced by the transient thermal flow. The sequence and magnitude of temperature changes (and therefore local dimensional changes) depend on the welding procedure and sequence. Due to the time limitation, only a simplified stress estimation was performed by the Mechanical Research Department. The detail of the analysis is enclosed as Appendix B.

The magnitude of the distortion as indicated in the first mock-up suggested that yielding occurred. Thus the yield stress of the actual roller path plate (26 ksi) was used in the calculation for the force level in the restraint plate. The calculation results suggested a restraint plate thickness of 4.8 mm (3/16 in) would be sufficient to transfer the load to the primary concrete. Also, the end of the roller path plate at the side plate should be supported by L3x2x3/8 angle brackets. Both the restraint plate and angle brackets should be bolted to the primary concrete every 216 mm (8.5 in.) using 19mm (3/4 in.) bolts. This configuration should not over stress the supporting concrete.

Appendix B also raised other concerns such as the accuracy of the stress estimation, the possibility of buckling of the side plate and the cracking at the weld metal/parent metal interface. Thus it was decided that a second mock-up was necessary to validate the estimated stress levels.

3.4 THE SECOND MOCK-UP

The second mock-up was instrumented to address questions such as those raised at the end of the last section. Instrumentation included load cells to measure the actual load on the roller path plate, and thermocouples to monitor the temperatures at various locations. To simulate closely the actual field conditions, the roller path plate was given a concrete backing. The concrete backing influenced the heat flow pattern in the mock-up and provided extra stiffness to the roller path plate to prevent backward bending of the plate.

Figure 13 shows the schematic layout of the second mock-up. Two 4.8 mm thick restraint plates, connected to I-beams located behind the roller path plate, provided restraint for distortion. Three load cells were used to monitor the load. It should be noted that, as in the first mock-up, the simulated roller path plate was made from 516 G70 material. Therefore, the load measured should be corrected for the lower strength UNS G10150 steel. Before the concrete was poured to form the backing, thermocouples were placed to monitor the temperatures reached during gouging and welding.

Gouging, welding and grinding were performed on the mock-up with optimized parameters. Beside monitoring the load and temperature, the time required to do the repair was also recorded. After the repair, residual stresses on the plate were measured using the blind hole drilling technique. Then two stress relief grooves, one on each side of the repaired patch, were made in an attempt to relieve the residual stresses. Finally the concrete was removed so that the roller path plate and the supporting I-beam could be examined closely.

3.4.1 Gouging, Welding and Grinding

Plasma arc gouging was done using the parameters listed in Table 2. As mentioned earlier, the gouged depth per pass was lower than that obtained in a smaller test plate. As a result, the profile shown in Figure 14a required up to three passes to esablish. The as gouged surface is shown in Figure 14b. Part of the gouged surface was cleaned thoroughly by grinding to reveal fresh metal, and other sections were cleaned less thoroughly. This was done to see how critical the cleaning process was for obtaining defect free weld deposits. No weld defect was attributable to insufficient cleaning.

An initial welding pass was made to partially fill the deeper region of the gouged surface. Then a second welding pass was done to fill up the remaining cavity. After the first welding pass, grinding of the start/stop regions of the weld beads, plus general cleaning were done prior to the second welding pass. During the second welding pass, three or four short stoppages were made for minor adjustments or examination of the weld deposits. These stoppages did not change in any significant way the interpass temperature. The welding parameters used were those listed in Table 3. The as deposited weld beads are shown in Figure 15. The as welded surface profile was very satisfactory in terms of bead shape and overall surface roughness.

The grinding operation was the most time consuming step. Using an air grinder partially supported by the P-KAT carriage, grinding was done manually. The resulted surface irregularities were considered to be unacceptable. (see Figure 16). The OHRD compact robot was than set up for a surface finish grinding step. The limited trial suggested that surface finish was much better, and definitely acceptable. Hence, it seems that manual grinding (which can use a large grinding wheel) should be used to remove the excess material and the compact robot should be used to provide a smooth surface profile. According to Automated Systems Unit personnel, the compact robot is able to maintain the alignment tolerance of 0.15 mm (0.006 in) over the length of the roller path. This would be an aspect that the compact robot has as an advantage over a mechanized system.

3.4.2 Temperature Measurements

A major concern was that the heat generated by the gouging and welding operations would overheat the concrete with detrimental effects. It was not clear what the critical temperature leading to concrete failure was. However, during previous meetings, the temperature of 200 C was suggested as acceptable. Thermocouples were embedded in the concrete, about 6 mm from the steel/concrete interface, and also on the back surface of the roller path plate, to monitor the

temperatures reached during the repair operations. Figure 17 shows the approximate locations of the thermocouples. Thermocouples 1 to 8 were at the steel surface, and Thermocouples 9 to 11 were in the concrete. It was found that Thermocouple 1 was damaged by the concrete pouring process.

Maximum temperatures were obtained in the final (widest) welding pass where welding was done practically in a continuous manner with only very short stoppages. The maximum temperature reached on the back surface of the roller plate was about 250 C. This temperature may not represent the actual peak temperature since it was found that the thermocouple was not placed directly beneath the path of the welding arc. The maximum temperature recorded by thermocouples in the concrete was 189 C, which was reached a few minutes after the welding arc passed directly over the thermocouple. Appendix C presents the temperatures recorded during the gouging and welding operations. There was no evidence that the heat from the repair operation caused any damage to the backing concrete.

The maximum temperature reached during repair depends on several factors. These include the heat input used in gouging and welding, continuous arc on time, and the efficiency of heat removal from the repaired region. In optimizing the welding and gouging parameters, the heat inputs were minimized. If welding was performed intermittently, allowing adequate cooling in between passes, the peak temperatures would be lower. Stoody Engineering suggested that the weld deposit be cooled by water spraying to lower the overall temperature. The present welding procedure concentrated the heat in a relatively small area. If welding could be done in a vertical up position, and spanned over a longer distance, the peak temperatures would also be lower. In the field, the actual roller path plate is larger and the heat transfer from the weld pool, aided also by the better air flow conditions, probably would be faster, lowering the maximum temperature.

3.4.3 Distortion

As in the first mock-up, perpendicular distances between sets of points were used as distortion indicators. In this case, however, the reference plane was set in front of the roller path plate. Figure 18 shows the locations of the monitoring points. Table 7 summarizes the changes in distances after the gouging and welding operations. The changes in distances were small, probably within the experimental resolution limit of the measuring technique. However, there was no doubt that distortion occurred as indicated by the significantly higher movement of the side plate. The positive values suggested the roller path plate curved backward. This apparent backward movement was a re ult of the distortion of a few parts of the mock-up.

The respective distances of the two restraint plates from the vertical I-beam were not the same, leading to an asymmetrical load distribution. This caused the restraint system to rotate slightly, bending the restraint plates. The movement of the plates were about 2 mm. The directions of the restraint plates' movements are shown in Figure 18. After the concrete was removed, close observations of the I-beam suggested a possible bending of the front flange and a slight twisting over the vertical axis of the web. The distortion of the I-beam, if any, was extremely small, in the range of about 1/2 mm to 1 mm. Again, the possible directions of movements of the I-beam

component parts are shown in Figure 19. Obviously, there is no simple interpretation of the distortion figures shown in Table 7.

After the grinding operation, and before the removal of the concrete backing, stress relief grooves were gouged out on each side of the repaired path. If the residual stress could be relieved, then the restraint system could be removed. There was a slight reduction (20%) of the load measured. However, after the restraint plates were removed there were movements of the side-plate . Table 8 summarizes the changes in the roller plate position before and after the removal of the restraint plates.

The measured distortion was small, all in the vicinity of a couple of millimetres. Thus the restraint system used successfully reduced the distortion to a low value. However, whether this magnitude of distortion is acceptable or otherwise is beyond the scope of this study.

3.4.4 Stresses in the Mock-Up

Three load cells were used to monitor the load over the 1.2 m long plate. Load readings were taken at 5 minute intervals during the gouging and welding operations, including stoppage intervals. The average load per unit length on the plate can be calculated by dividing the total load of the three cells by the length of the plate. The load readings are collected in Appendix D, and Table 9 is an extract from Appendix D showing peak load readings by any load cell, and load readings after each gouging or welding pass, as well as the final load readings after the formation of the stress relief grooves. The positive load reading corresponded to a tensional load on the roller path plate.

The total load on the plate increased with additional passes of gouging or welding. This was expected as additional gouging or welding introduced more localized heating. The maximum total load occurred after the finish of the welding operation and the plate had cooled down. The measured average load on the plate was 29800 lb/ft. If the plate had a yield strength of 26 ksi (as is the case in Abitibi), the load would become 18000 lb/ft, as predicted in the stress analysis. In gouging out the stress relief grooves, the load initially increased, again due to additional heating. Only when the groove depth reached about 20 mm did the load start to decrease. This was due to the yielding of the remaining material beneath the groove. However, the load reduction was only about 20% and could not eliminate further distortion when the restraint plates were removed.

While the average load over the plate is of great significance, the local stress level can be more critical. The highest load reading of 45,200 lb was recorded by load cell #3 during the final welding pass. It is not possible to give an accurate estimate of the localized stress due to the uncertainty of the monitoring range of the load cell. However, judging from the fact that distortion occurred and there was possible damage to the I-beam, yield stress levels were reached locally during the repair operation.

Although the average load was well predicted by the stress calculation done by the Mechanical

Research Department, the localized transient stress could not have been estimated. Such transient stress could be reduced by minimizing the temperature during the repair operation. One way to do this is by specifying a low interpass temperature with prolonged cooling in between passes. Of course, the critical interpass temperature was not known and could not be estimated here. A more practical way may be the use of external cooling system to control the temperature during the repair operations.

The residual stresses in the roller path plate after the welding and grinding operations were measured. The Blind Hole technique was used to measure the residual stresses in various locations on the roller path plate. Figure 20 shows the location of the holes drilled. Table 10 summarizes the residual stress levels measured. The residual stress levels on the weld metal were quite high, reaching the yield stress level of the weld deposit at some locations. It seems that there was a trend of higher residual stress at the upper part of the plate. On the parent material zone, the highest residual stress occurred near the weld metal/parent metal interface. At these locations, the residual exceeded the yield stress of the parent metal. As expected, the residual stress level dropped at locations further away from the interface.

Although the residual stress levels were high, there was no cracking observed, even at the interface regions, as shown by the results of a liquid penetrant inspection. A side bend test was performed on a specimen machined from a weld coupon, and no cracking was observed. The stress was accommodated by complex yielding of the materials without generating any discontinuity.

3.4.5 Repair Time Requirement

The repair procedure included three operations; gouging, welding and grinding. To repair a 5 inch wide patch, the time requirement is estimated as follows:

Gouging:	Preparation	1 hr.
	Gouging	5 min/ft
Welding:	Preparation	1 hr.
	Welding	30 min/ft
	Stoppage	15 min/45 min of welding
Grinding:	Preparation	1 hr.
	Grinding	3 hr/ft

Hence, the time required to do a 30 ft length of roller track plate, with two gouging passes and two layers of weld deposits, would be about 137 hr. A minimum of a two man team is required, but additional team members would have only marginal effect on the time requirement. Also, the time estimate excludes the time required to build the restraint system.

Assuming it takes three days and a five men crew to construct the restraint system, and at

$60/hr, the labour cost will be $9,000. Assuming the repair takes 180 hours, allowing extra time for touch up work and unforseen stoppages, with a two men crew, the labour cost will be $21,000. The cost to repair a headgate path with two roller track plates would be about $60,000. Even after adding engineering and materials cost, the cost of repairing a headgate unit would be less than $100,000.

Although using the welding technology to repair the headgate roller path plate is economically attractive, there are some technical uncertainties. These include the maximum temperature and stress level in the concrete and its supporting structure, as well as the tolerance on distortion. The long term effects of the presence of residual stress in the roller path plate, the restraint system, and the surrounding concrete structure are also not known.

4.0 DISCUSSION AND RECOMMENDATIONS

The mechanized system used in this feasibility study adequately handled the repair. However, some aspects can be improved. Using the mechanized system, the gouged depth and the weld deposit thickness cannot be controlled. Variation in the gouged depth or the weld deposit thickness occurred partly because the arc length cannot be kept constant. Automatic voltage control systems, such as the one employed in the OHRD compact robot, are available for maintaining a constant arc length. The use of such systems will lead to a better surface profile and will minimize the amount of grinding required. The surface finish and alignment tolerance obtained by the manual grinding process is not satisfactory. The robot can provide a much better surface finish, although some of the control software needs to be improved.

The welding procedure depends very much on the filler material selection. The current wire is very compatible to the parent material. The deposited material will have good corrosion resistance and wear properties. The deposited material will have minimal deformation under load due to its high work hardening coefficient. Therefore, the chance of interface cracking at the base metal/weld metal interface is very small, as suggested by Dr. G. Bellamy. If a filler metal which gives a less fluid weld pool is selected, the welding procedure may be changed such that welding need not be confined to the horizontal position with upward progression, the resulting stress distribution and distortion may be quite different. For example, if welding is done in a vertical up position over a large length, the degree of heat concentration will be much lower, probably reducing distortion.

Using the current distortion control system, the distortion is reduced to a low level, at the expense of high residual stress in the roller path plate. The residual stress measured after the repair reached the yield stress level. Gouging stress relief grooves did not sufficiently reduce the residual stress such that the distortion control system can be removed. There are two concerns. First, it is not known how the residual stress will be redistributed after loading by the passage of the wheels. Such redistribution may cause serious distortion of the structural I-beam. Secondly, the maintenance of the distortion control system becomes an important issue, as failure

of the system may lead to sudden movements of the headgate assembly. These shortcomings must be resolved before the technology can be applied.

Creation of stress relief grooves, as suggested by the Mechanical Research Department, after the repair was done did not reduce the stress to a satisfactory level. There is no obvious reason for the failure of this stress relief. However, it may be that the grooves should be created prior to the repair work, allowing localized yielding during the gouging and welding operations. Such localized yielding generally minimizes residual stress. The appropriate depth of the stress relief grooves needs to be assessed.

As mentioned, there are observations suggesting the distortion of the mock-up I-beam due to the repair operation. Although the actual I-beam in a headgate roller path plate is larger and stiffer, this observation requires appropriate caution. Assuming the I-beam was distorted, the factors contributing to the distortion will be of great interest. Specifically, the contribution, if any, of the design of the distortion control system would directly influence the applicability of the welding technology in the repair of the head gate.

This feasibility study has provided valuable information on the repair option in headgate roller path plate repair. This study was made under the assumption that gouging and welding will be used in extensive repair covering the whole length of the plate. Under this scenario, a vast amount of welding is necessary and the likelihood of distortion will be very high. The amount of distortion is expected to increase with the amount of welding. Although distortion can be controlled, as shown in this study, the uncertainty in the residual levels and the subsequent possible redistribution of the stress demand caution in the general application of the technology. However, the economic aspect of the approach remains attractive, and may warrant further development of the technology.

It is recommended that the welding option should not be applied before further development of the technology. Further studies should include a look at the effects of various welding procedures. As mentioned, a change of filler material may allow welding in the vertical up position with stringer beads. This will significantly lower the interbead temperature and heat flow pattern. The effect of alternative distortion control systems should also be included. From a practical point of view, it is likely that the success of the welding option would be found in limited repair cases. Future development should emphasize this aspect.

5.0 CONCLUSIONS

This feasibility study has provided valuable information on the welding option for headgate roller plate repair. The following conclusions can be drawn:

1. The gouging procedure developed provided proper surface preparation for the subsequent welding build up. The welding procedure gave an excellent rebuilt surface with good surface profile and penetration.

2. The first mock-up provided information for the estimation of stress levels and the design of a distortion control system. The calculated stress was verified by the measurements made in the second mock-up.

3. The distortion control system in the second mock-up did not eliminate distortion completely. However, the distortion observed was small. There were residual stresses, up to the yield stress level, present in the plate.

4. There were observations suggesting distortion of the I-beam. The amount, if any, was small and within the limit of experimental errors of the measuring technique used.

5. Due to the distortion observed, high levels of residual stresses, and the uncertainty in the possible redistribution of the stress, the welding option for roller plate repair is not recommended at this time.

6. The welding technology for repair warrants further development. However, future development should be focused on applications in localized limited repair.

ACKNOWLEDGEMENTS

The initiation of this project, by Mr. M. Tinkler is acknowledged. The assistance provided by Mr. M. Flaman, Mr. B. Teper, Mr. W. Mika and the technical staff of the Mechanical Research Department, in stress analysis, and the design of the second mock-up is deeply appreciated. Technical discussions with Dr. S. Lawson, Mr. J. Galloway and other staff members in the Metallurgy Section are hereby acknowledged.

Reviewed by

W.H.S. Lawson
Supervising Engineer
Metallurgy Section

Prepared by

Thomas Lau
Engineer-Welding
Metallurgy Section

Murray Mathers
Technician-Welding
Metallurgy Section

Approved by

J. Brown
Manager
Metallurgy Research Dept

TL:MM:dw

TABLE 1

COMPOSITION OF STOODY 110-0
(COURTESY OF STOODY ENGINEERING)

Typical Wire Composition (%)						
Cr	Mn	Mo	Ni	Si	C	Fe
18.0	15.0	0.7	0.7	0.4	0.3	Bal.

TABLE 2

RECOMMENDED GOUGING PARAMETERS

Current	Inclination Angle (W.R.T. Vertical)	Standoff[1]	Air Pressure
90 (Amps)	35°	15 mm	80 psi
Weave Speed (Setting)	Weave Dwell Time	P-Kat Speed (Setting)	
26.4 mm/s (25)	1/8 Second[2]	12.8 mm/s (30 I.P.M.)	

Notes:

(1) Heat shield to workpiece distance
(2) Minimum response time for P-kat

TABLE 3

RECOMMENDED PARAMETERS FOR WELDING OPERATION

<table>
<tr><td colspan="3">Current Settings</td><td>Peak Voltage Setting</td><td>Pulses/s</td><td>Wire Speed (Setting)</td></tr>
<tr><td>Background
26A</td><td>Peak
530A</td><td>Avg.
185A</td><td>35.3 V</td><td>120</td><td>89 mm/s (210)</td></tr>
<tr><td colspan="2">Inclination(1)
Angle
15°</td><td>Contact Tip
to Workpiece
12 mm</td><td>Weave Speed
3.9 mm/s</td><td>Dwell Time
3.2 s</td><td></td></tr>
<tr><td colspan="3">P-kat Travel Speed
(Setting)
1.7 mm/s
(3.9 I.P.M.)</td><td></td><td></td><td></td></tr>
</table>

Notes:

(1) With Respect to Horizontal

TABLE 4

GOUGING PARAMETERS USED FOR THE FIRST MOCKUP

Current 90A	Inclination Angle(1) 36°	Standoff(2) 15 mm	Air Pressure 79 psi
Weave Speed (Setting) 26.4 mm/s (25)	Dwell Time ≈ 1/8 s	Kat Travel Speed 8.3 mm/s	Progression Downward

Notes:

(1) With respect to vertical
(2) Heat shield to workpiece distance

TABLE 5

PARAMETERS USED FOR WELDING OF THE FIRST MOCKUP

Current Settings			Peak Voltage Setting	Pulse Rate	Wire Speed (Setting)
Background	Peak	Avg.			
35A	650A	148A	35.0 V	60/s	72 mm/s (170)
Inclination Angle		Contact Tip to Workpiece	Weave Speed	Dwell Time	Kat Travel Speed
1st Bead	Balance				
0°	15°	12 mm	3.3 mm/s	3.2 s	2.2 mm/s

Notes:

(1) With respect to horizontal

TABLE 6

DISTORTION OF THE FIRST MOCKUP
(Measurements in mm from Initial Position)

As Gouged Distortion Vert. Location	Horiz. Location/Point Measurement							
	A	B	C	D	E	F	G	H
1	1	1.5	1	3.5	0	0	0	0
2	1	0.5	6.5	5	0	0	0	0
3	1	2	0.5	6	0	0	0	0
4	0.5	1.5	1.5	6.5	0	0	0	0
5	1.5	2	1	4	0	0	0	0
6					0	3	6	

As Welded Distortion	Horiz. Location/Point Measurement							
	A	B	C	D	E	F	G	H
1	4	3	3	6.5	0	0	0	0
2	4	2.5	8.5	10.5	0	0	0	0
3	3.5	0	5.5	11	0	0	0	0
4	3	1	5	10	0	0	0	0
5	1.5	0.5	2.5	5	0	0	0	0
6					0.5	7	14.5	

TABLE 7

DISTORTION OF THE SECOND MOCKUP
(Measurements in mm from Initial Position)

As Gouged Distortion Vert. Location	Horiz. Location/Point Measurement					
	A	B	C	D	E	F
1	1	0	1	0	3	5.5
2	0.5	-1	-0.5	0		
3	0.5	-1	0	0		
4	0	-0.5	0	-0.5		
5	2	0	1.5	-1.5		

As Welded Distortion	Horiz. Location/Point Measurement					
	A	B	C	D	E	F
1	2	1	1	1	6	11
2	1	0.5	1	1		
3	1.5	0	1	1		
4	1	1	1	0		
5	2.5	2	2.5	-1.5		

TABLE 8

NET DISTORTION OF THE SECOND MOCKUP AFTER ATTEMPTED MINIMIZATION STEPS (Measurements in mm from Initial Position)

As Ground Distortion Vert. Location	Horiz. Location/Point Measurement					
	A	B	C	D	E	F
1	2	1.5	1.5	1.5	5.5	11
2	1	0	1.5	1		
3	1.5	0	2	1		
4	0.5	1.5	0.5	0		
5	2	2.5	2.5	-0.5		

As Ground Distortion with Stress Relief Grooves Gouged	Horiz. Location/Point Measurement					
	A	B	C	D	E	F
1	3	4	1	-0.5	5	9.5
2	2	2.5	1.5	1.5		
3	2	2.5	2.5	1.5		
4	2.5	3.5	1	0		
5	4	5	2	0		

Distortion After Removal of Restraints	Horiz. Location/Point Measurement					
	A	B	C	D	E	F
1	2	1	0.5	-0.5	7.5	16
2	1.5	0.5	2.5	0.5		
3	1.5	0	2	1		
4	1.5	1.5	0.5	-1		
5	4	2.5	4.5	0		

TABLE 9

SELECTED LOAD CELL READINGS
FROM APPENDIX D

Operation	Load Cell (K.lb)			Total Load
	#1	#2	#3	
1st Plasma Gouging Pass	7.59	1.56	1.15	10.3
2nd Plasma Gouging Pass	16.58	10.66	21.21	48.44
3rd Plasma Gouging Pass	23.35	17.21	25.40	64.97
1st Welding Pass	26.55	22.05	30.83	79.43
2nd Welding Pass-Single Load Cell Maximum Reading	32.33	29.1	45.22	106.64
End of 2nd Welding Pass	43.46	33.12	40.86	117.43
After Gouging of Stress Relief Groove	37.60	23.85	25.98	87.44

TABLE 10

RESIDUAL STRESSES OF MOCKUP #2

Location	Yield	Horizontal Stress (MPa)	Vertical Stress (MPa)	Shear & Stress (MPa)
1	696	297	314	-4
2	696	207	283	-50
3	696	300	592	-79
4	696	341	274	15
5	220	Yield Stress at Measurement Location		
6	220	95	10	-24
7	220	90	10	-4
8	220	98	122	-4
9	220	19	119	28
10	696	Yield Stress at Measurement Location		

Notes:

* The stresses are reported as positive=tensile.
* If a calculated residual stress is in excess of the yield strength of the steel, the result is simply listed as being in excess of yield.
* Nominal yield strength values used: CS1018 - Hot Rolled - 220 MPa
  Stoody 110 - 696 MPa
* Location numbers as shown on Figure 20.
* Vertical stress is stress acting along a vertical line - ie. along the line of the weld. Horizontal stress, therefore, acts along the line of the weld beads.

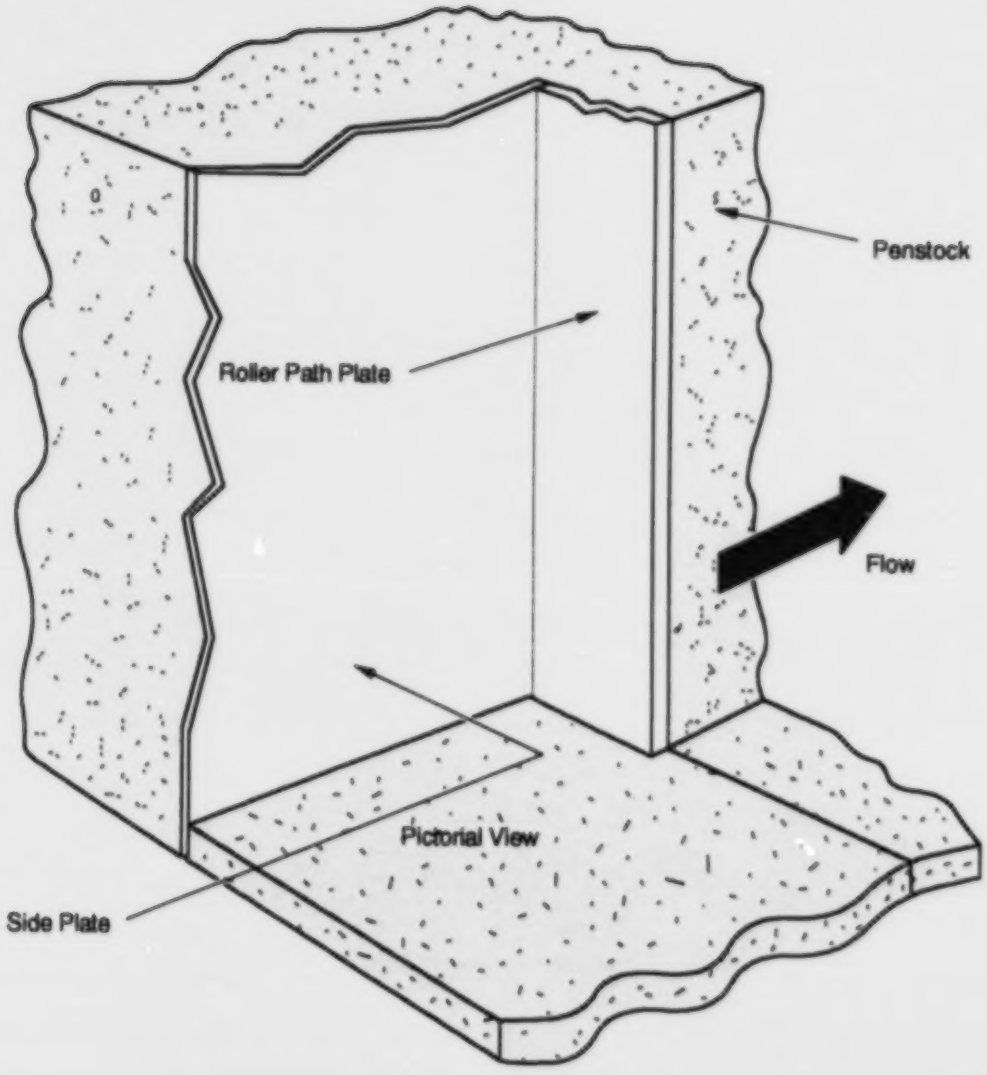

FIGURE 1

PICTORIAL VIEW OF ROLLER PATH

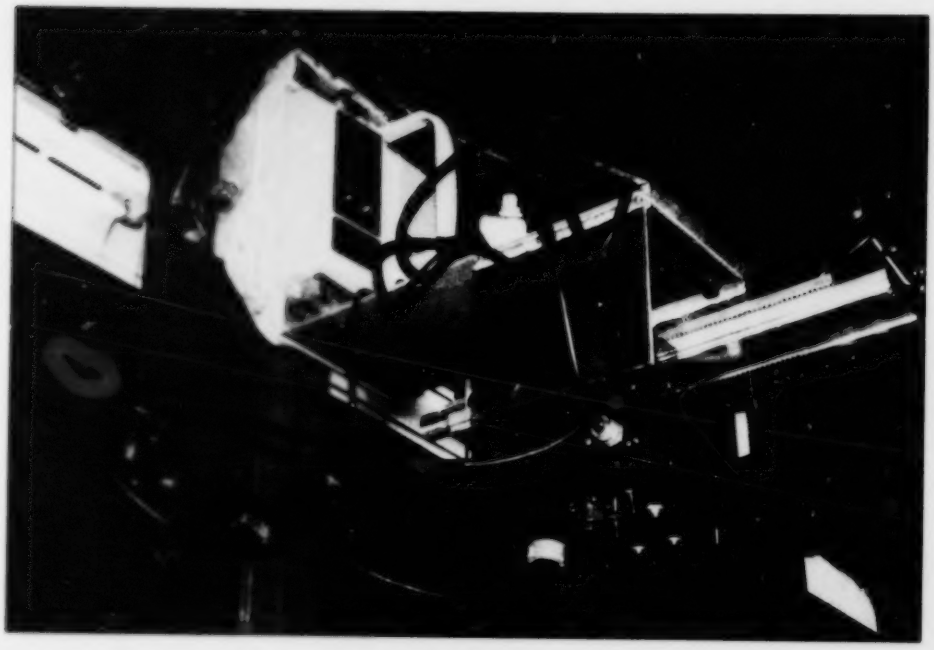

(a)

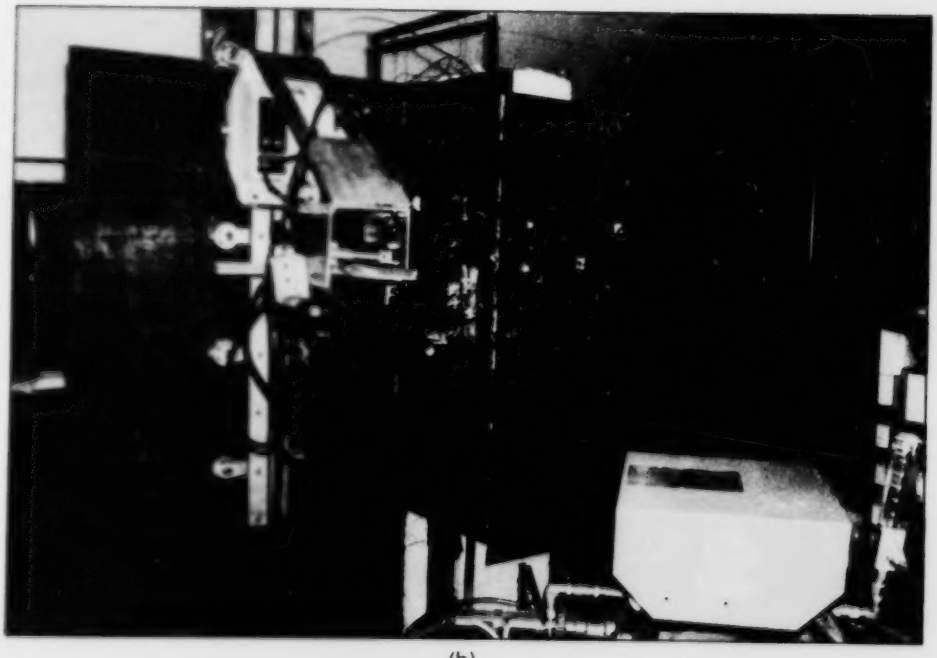

(b)

FIGURE 2

MECHANIZED GOUGING/WELDING SYSTEM
(a) SHOWING P-KAT/BUG-O ASSEMBLY
(b) WITH GOUGING HEAD ATTACHED

90-337
184643-B26-RD

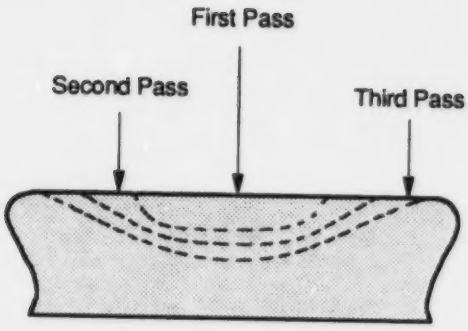

Figure 3a Transverse

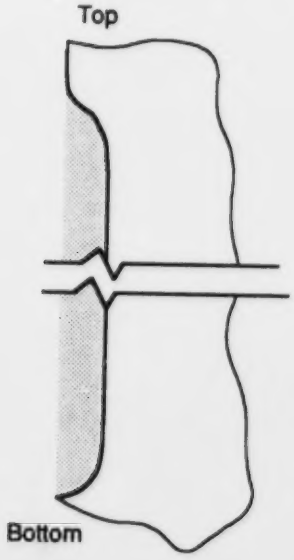

Figure 3b Longitudinal

FIGURE 3

AS GOUGED PROFILES

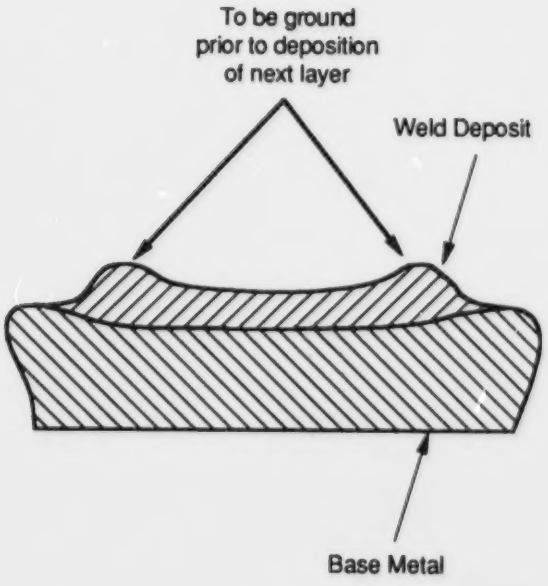

FIGURE 4

A BEAD PROFILE

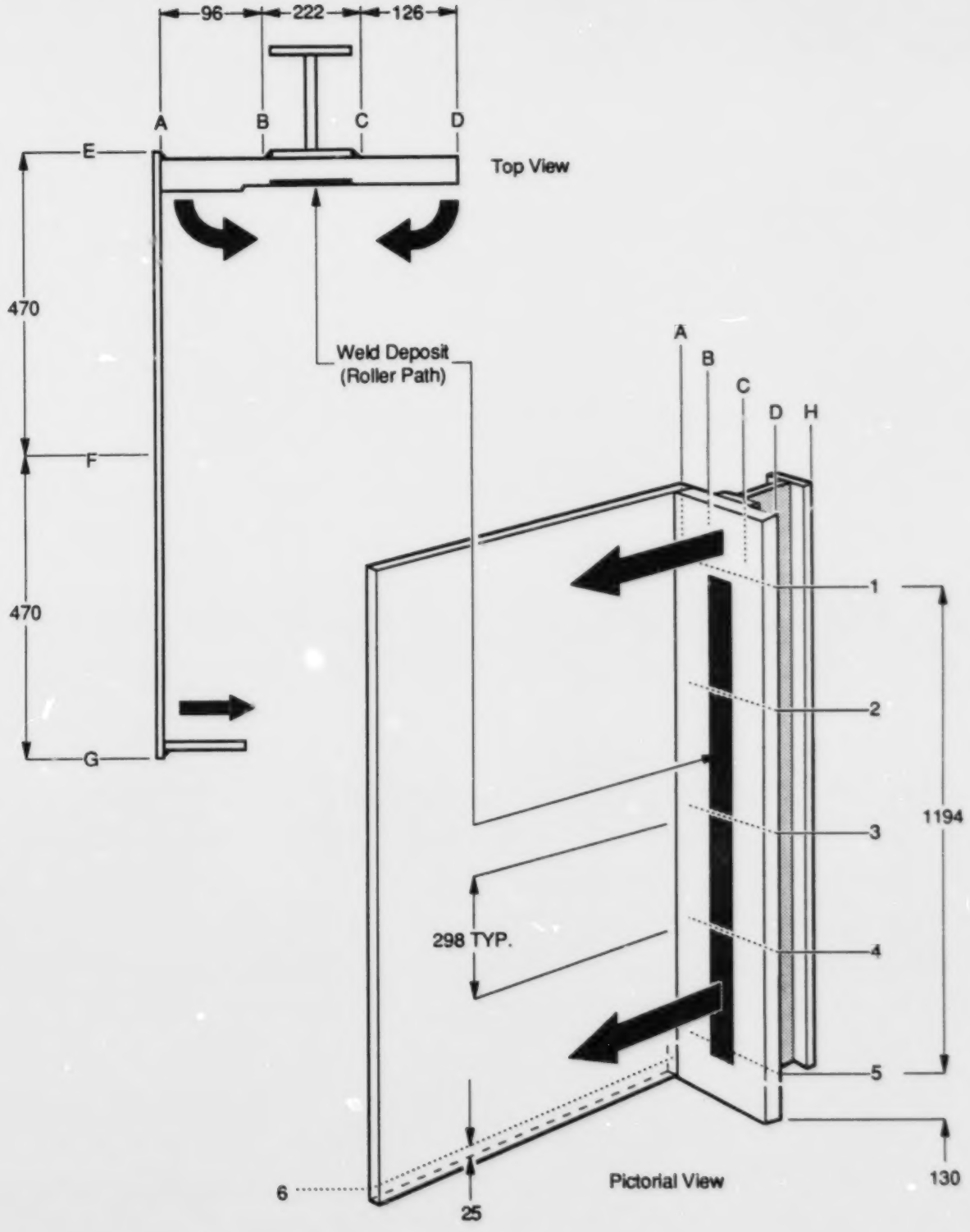

FIGURE 5

DISTORTION MEASUREMENT POINTS ON ROLLER PATH
MOCKUP #1 ALL DIMENSIONS IN MILLIMETERS

90-337

184587-F24-RD

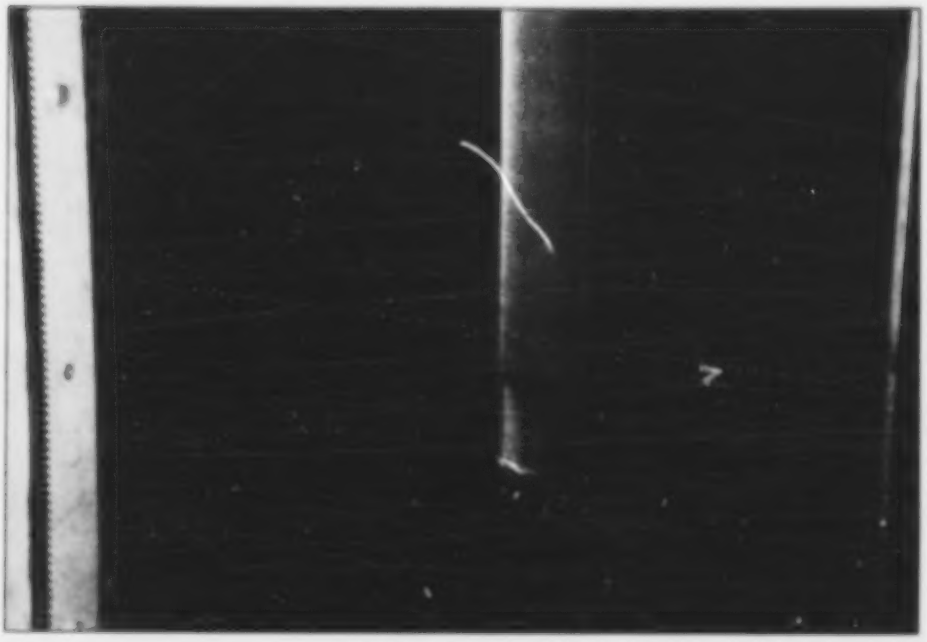

(a) First Gouge Pass

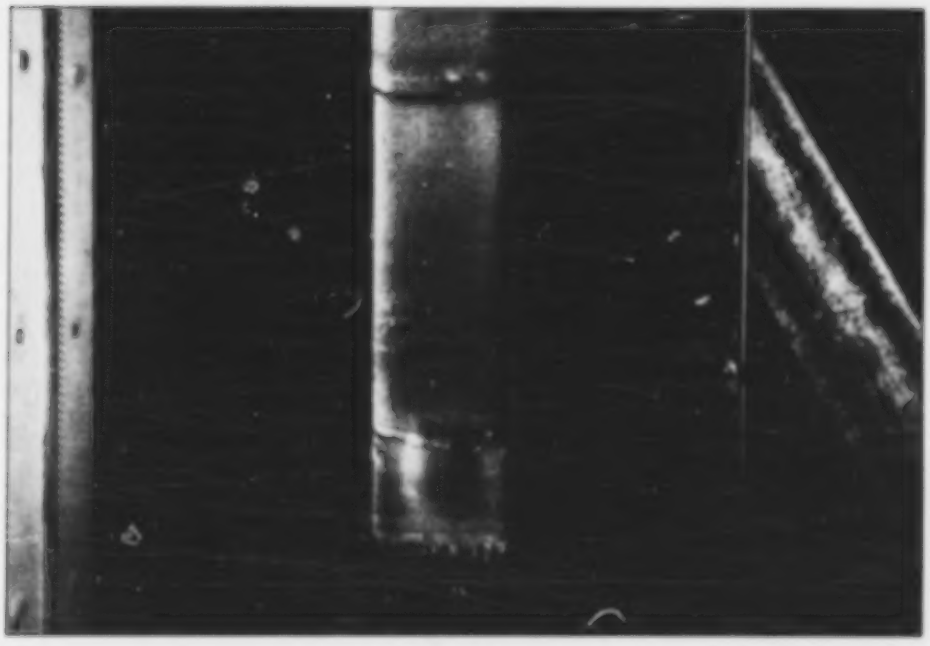

(b) Final Gouge

FIGURE 6

AS GOUGED SURFACE APPEARANCE

FIGURE 7

AS WELDED SURFACE APPEARANCE

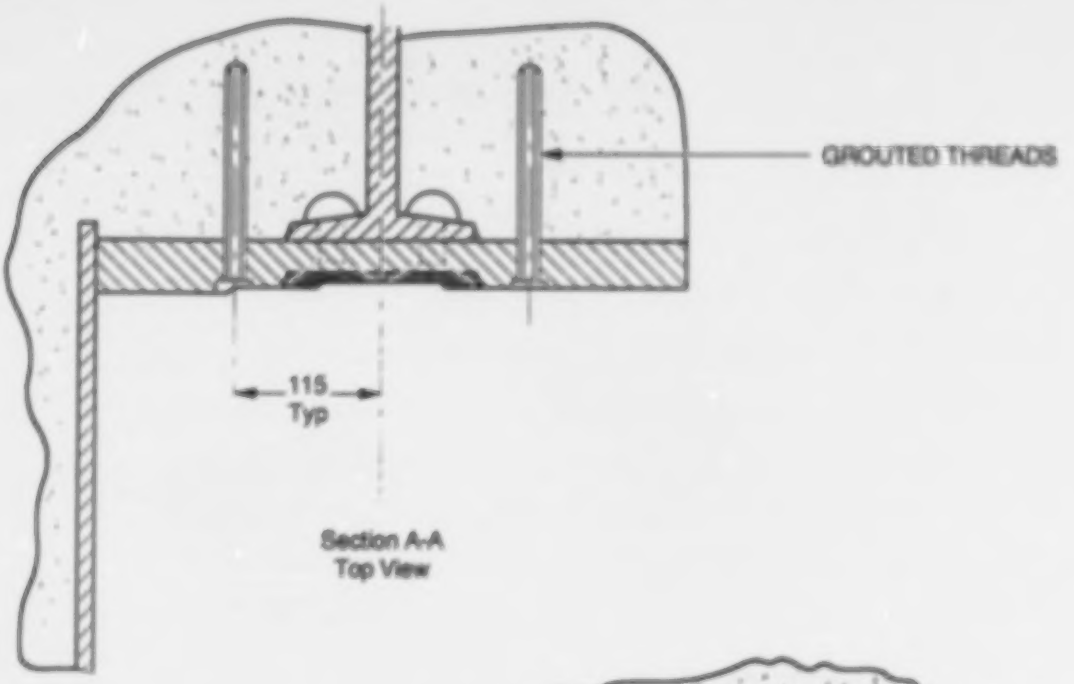

Section A-A
Top View

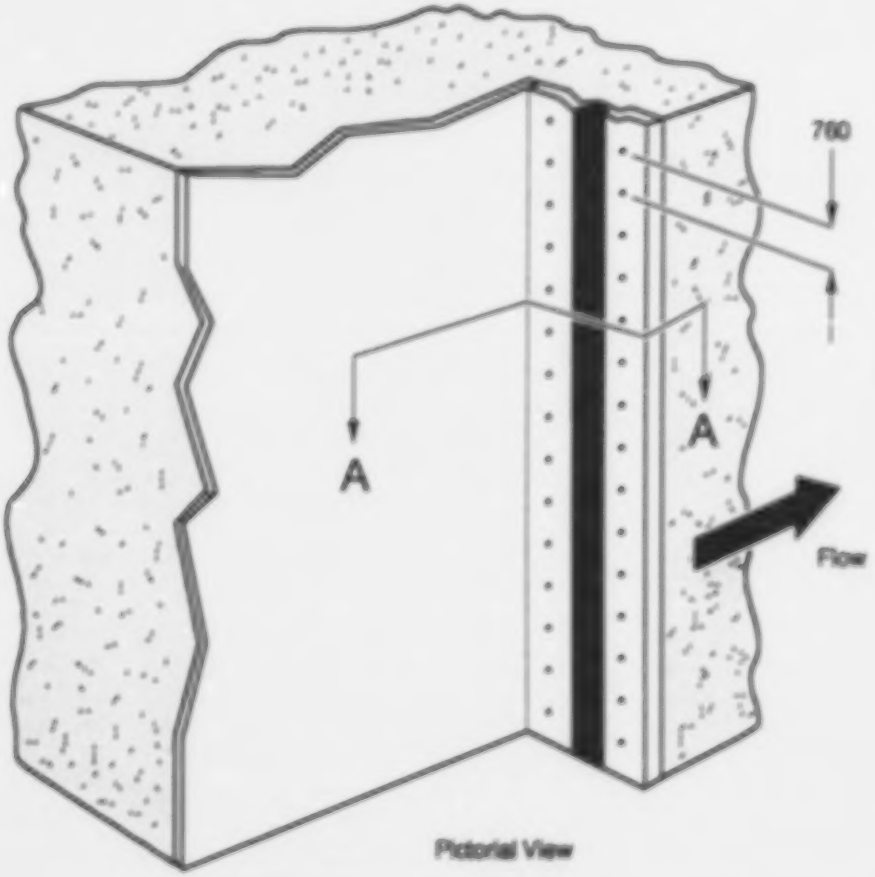

Pictorial View

Note: all dimensions in mm

FIGURE 8

PROPOSED DISTORTION CONTROL FOR ROLLER PATH WELD REPAIR USING ANCHOR BOLTS

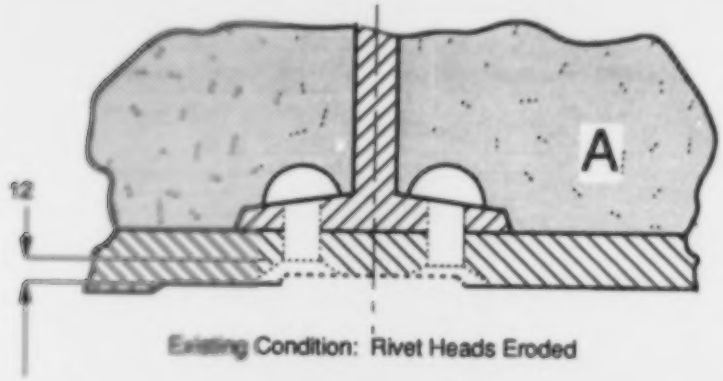

Existing Condition: Rivet Heads Eroded

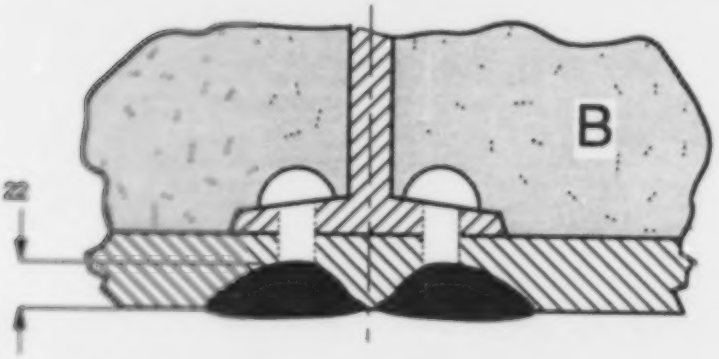

Following Plasma Gouging & Welding of the Rivet Heads

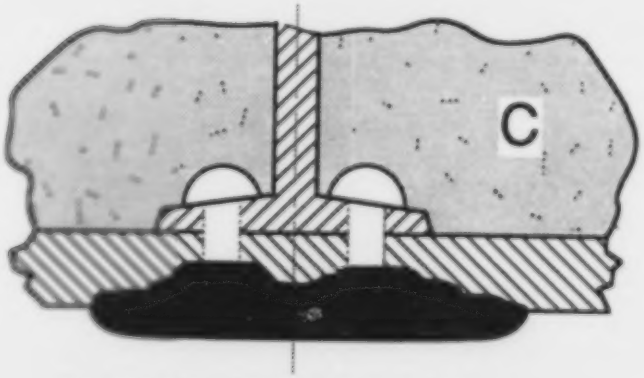

Following Complete Roller Path Weld Repair

(dimensions in mm)

FIGURE 9

SECTION A-A OF FIGURE 8:
PROPOSED DISTORTION CONTROL FOR ROLLER PATH WELD REPAIR USING GOUGED AND WELDED RIVET HEADS

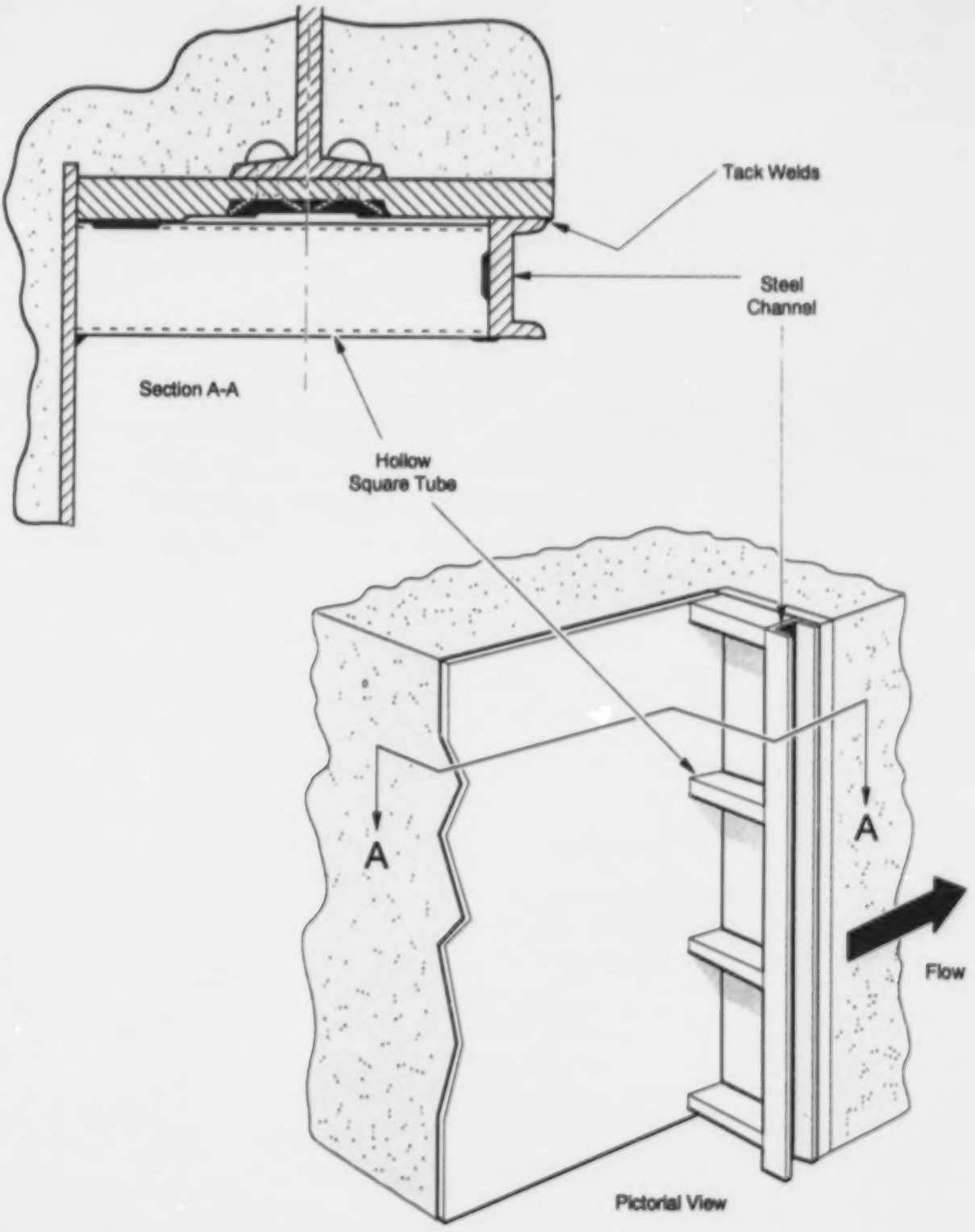

FIGURE 10

PROPOSED DISTORTION CONTROL FOR ROLLER PATH WELD REPAIR USING TEMPORARY STRUCTURAL STIFFENING MEMBERS

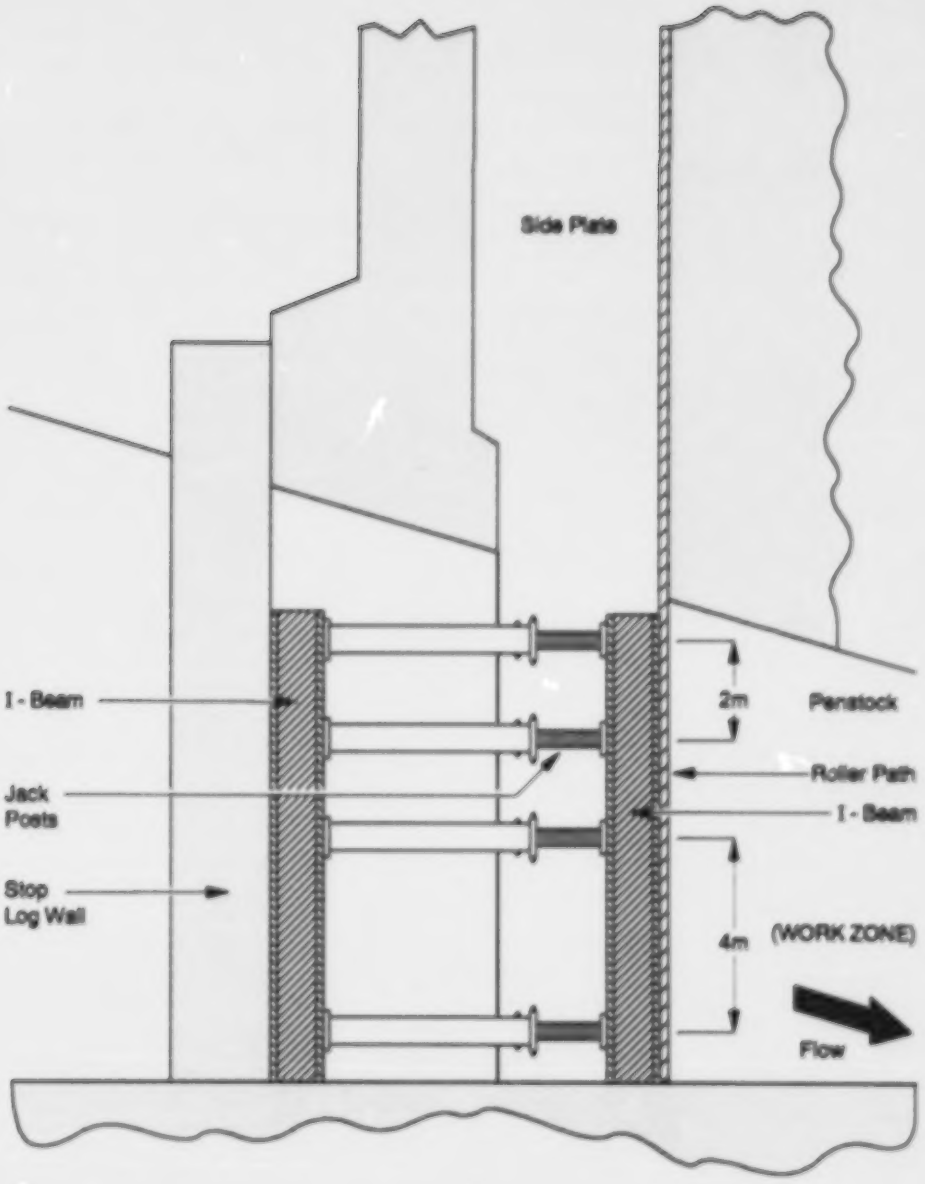

FIGURE 11

**PROPOSED DISTORTION CONTROL FOR ROLLER PATH
WELD REPAIR USING JACK POST SUPPORT FROM STOP LOG WALL**

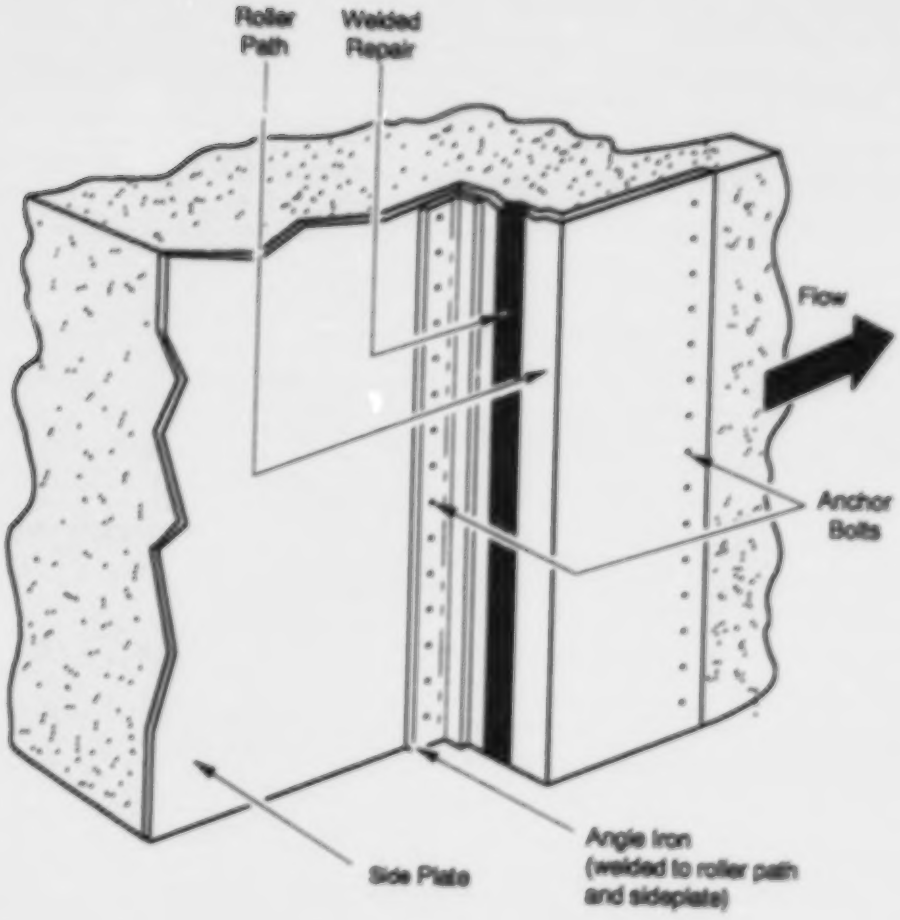

FIGURE 12

PROPOSED DISTORTION CONTROL FOR ROLLER PATH WELD REPAIR USING LOAD TRANSFERRING SIDE PLATES

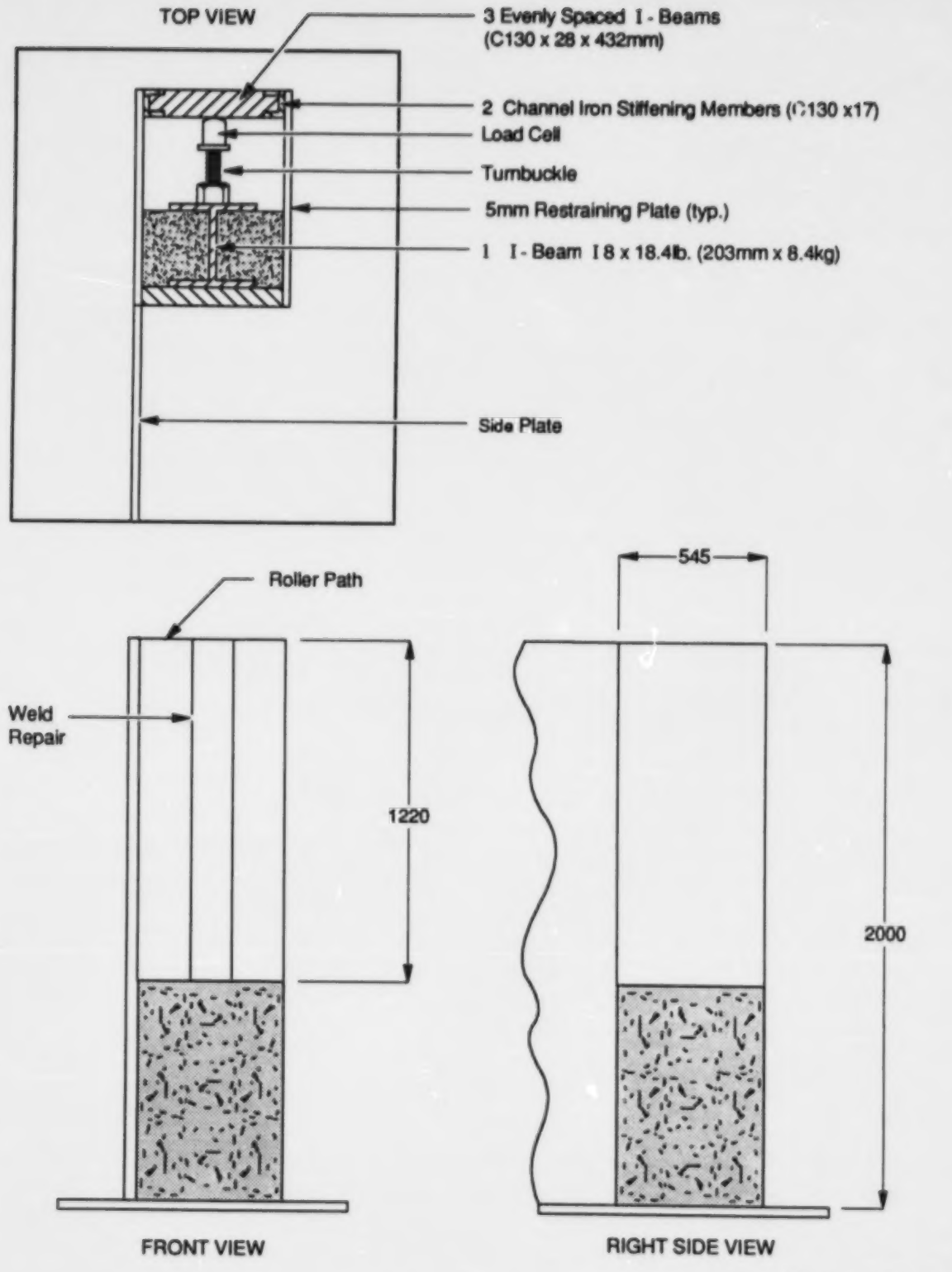

FIGURE 13

CONCEPTUAL DIAGRAM OF MOCKUP #2

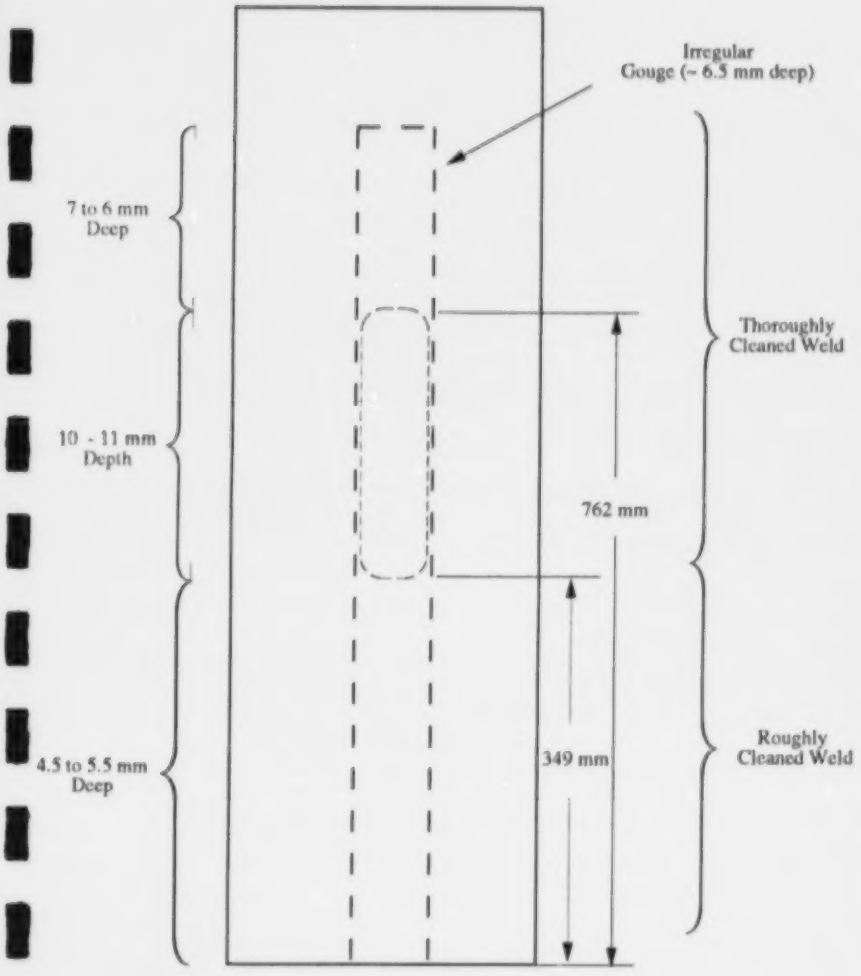

FIGURE 14(a)

PROFILE OF ROLLER TRACK PLATE AFTER GOUGING

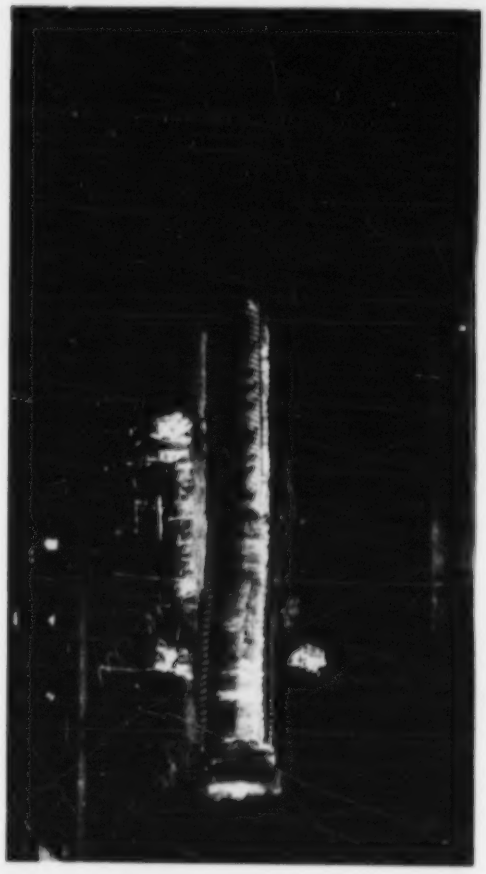

FIGURE 14(b)

AS GOUGED SURFACE

FIGURE 15

AS WELDED SURFACE

FIGURE 16

AS GROUND SURFACE (MANUALLY GROUND)

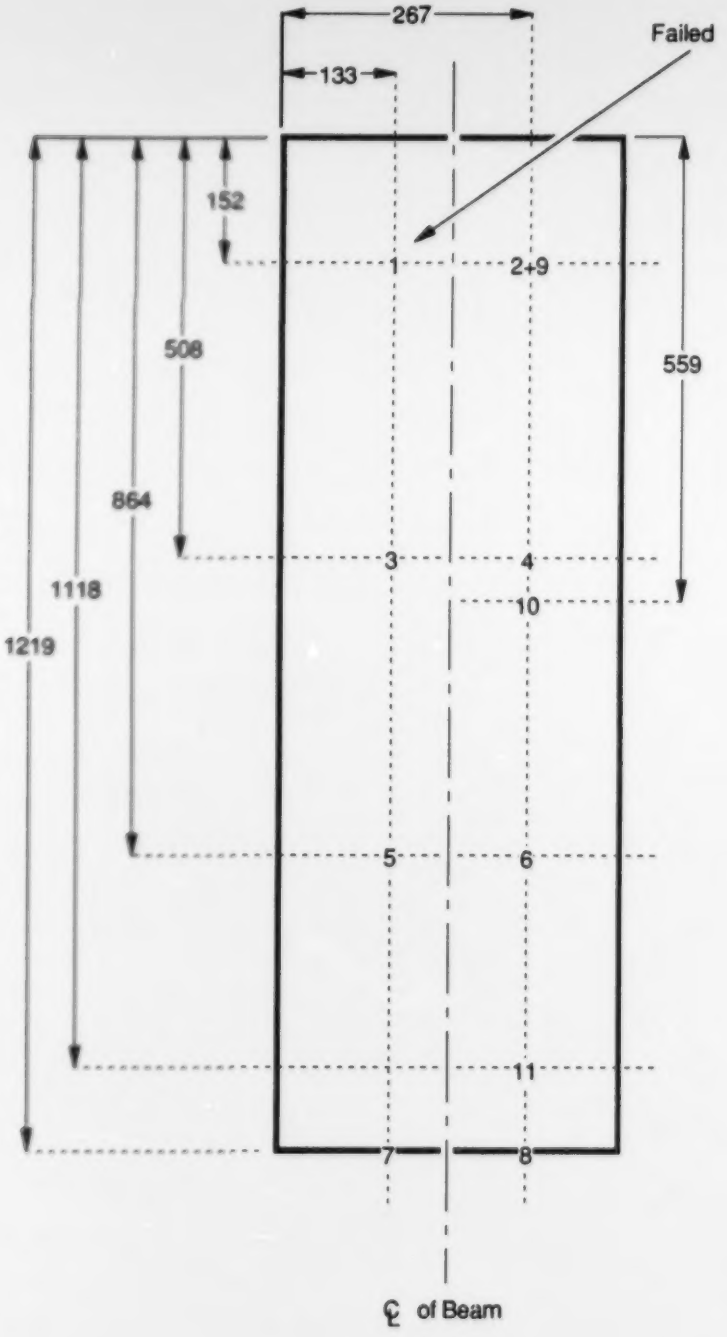

(dimensions in mm)

FIGURE 17

LOCATIONS OF THERMOCOUPLES

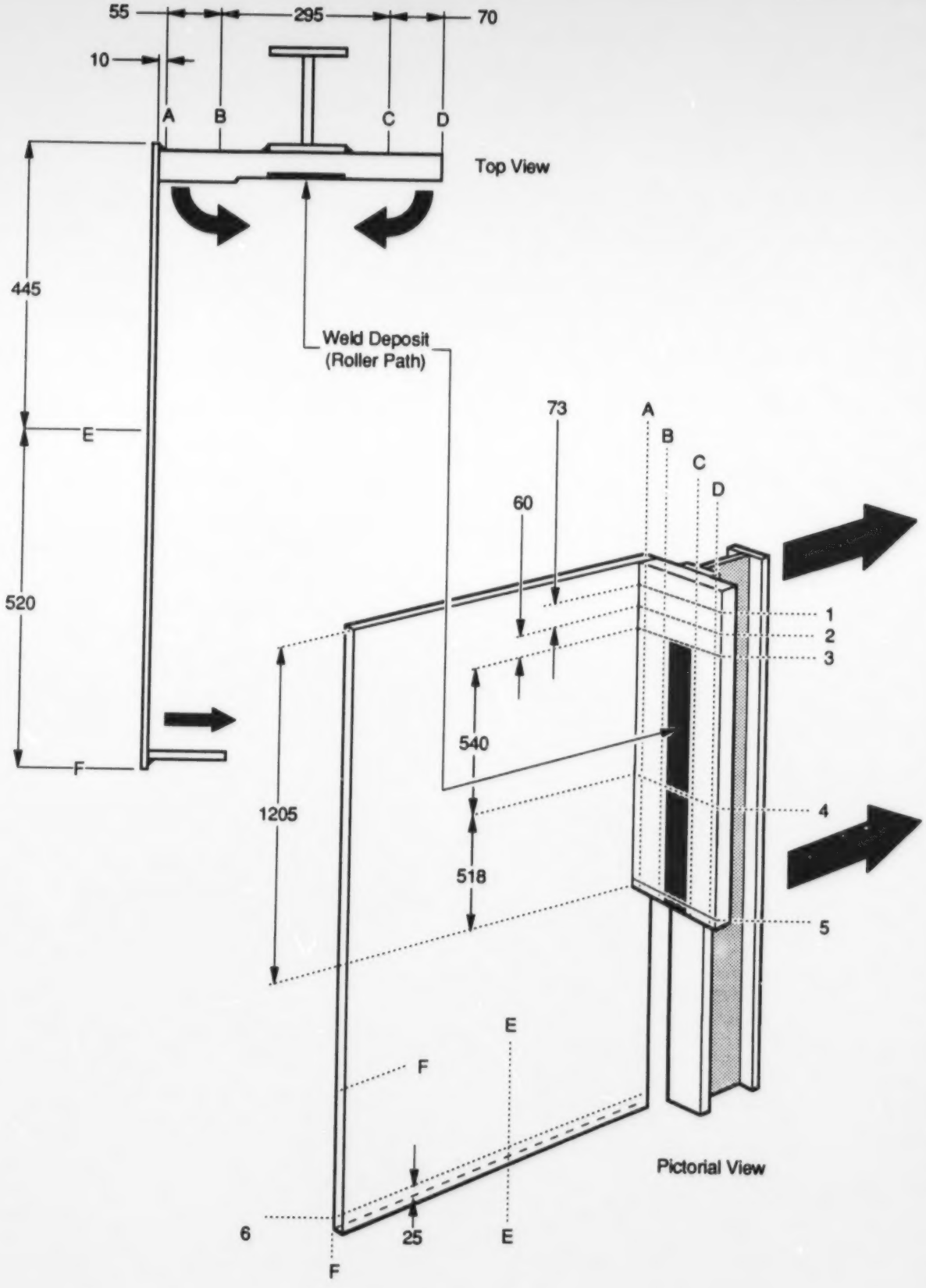

FIGURE 18

DISTORTION MEASUREMENT LOCATIONS ON ROLLER PATH MOCKUP #2
(all dimensions in millimeters)

184585-F24-RD
90-337

FIGURE 19

PROBABLE DISTORTION OF THE I-BEAM

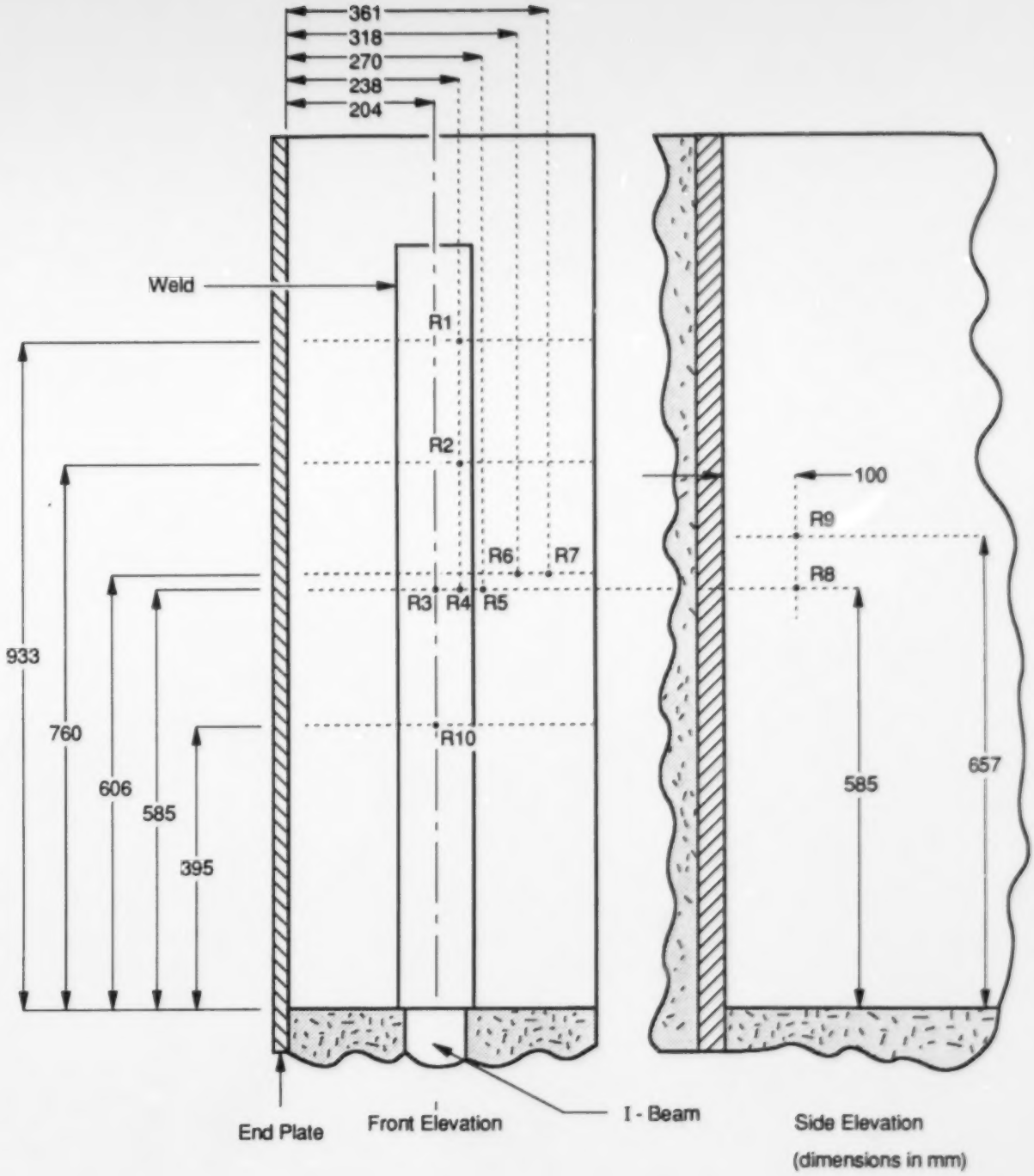

FIGURE 20

ABITIBI CANYON-HEAD GATE TRACK REPAIR SIMULATION
LOCATIONS OF RESIDUAL STRESS MEASUREMENT ROSETTES

APPENDIX A

January 16, 1990

To: G. Bellamy

Subject: Comments re Repair of Headgate Roller Paths

We have been asked to recommend appropriate weld metal composition to effect the buildup of the wear track caused by the wheels of the headgates at Abitibi Canyon GS. The requirement is that a material be selected which has superior resistance to the type of damage observed, so that such a repair will not be required again over the life of the station.

The following are relevant points of information gathered during discussions about the problem, which impact on our material selection decision:

- Although the observed wear (~1/4" depth) is relatively small considering the 40 year life of the station, it is possible that most of this happened early on before the brass seal plates lost their ability to deflect (because of cinder buildup behind them), likely resulting in off-loading of the wheels. Once the seals are replaced, full wheel loading (estimated at 100 ksi) will be re-established on the roller path. Therefore, something more resistant than the existing 1015 plate steel is required.

- The wear mechanism is likely a cycle of corrosion product and barnacle buildup, which are then worn away by the wheel load. This exposes fresh metal for another cycle of oxidation and barnacle growth, etc. Consequently, it is important that a corrosion resistant alloy be selected. An alloy resistant to marine life growth (eg copper containing) would also be desirable.

- Because of the high compressive load, corrosion resistance is not enough. A common austenitic stainless steel, while strongly resistant to corrosion, was found to have insufficient strength to resist complete plastic deformation under load. Therefore, adequately high yield stress is a requirement.

- The need for surface hardness is a question. Because of the hardness of the wheels (said to be >500 Brinell) something harder than the 1015 would be considered appropriate to resist metal-to-metal wear. But they are rolling wheels, so how much wear is expected under normal operation? A recommendation is to reduce the hardness of the wheels substantially, so that these become the consumable in future (they are much easier to replace than the concrete embedded roller plate).

- It must be recognized that there are practical problems in effecting the proposed repair. In particular, there will be a lot of moisture around (50' below the river bed in the high humidity of middle of the summer). Also, the possibility of generating any significant level of

preheat in the base plate is not great. Therefore, a welding consumable susceptible to hydrogen cracking would not be a good idea. Under the loads envisaged it is a concern that a weld deposit containing cracks would be likely to spall off. This would rule out the use of a martensitic stainless steel consumable such as 410 or 420, which normally requires relatively high preheat (eg 350-450F) to minimize hydrogen cracking potential.

From the above, the number of potential alloys for this application is narrowed down to only a few. These are noted below, with annotations, and commercial descriptive literature is attached:

Stellite 6 - This appears to be a good choice, satisfying pretty well all the property requirements. Cost is high, however. Typically expect to pay about $50/lb for this stuff in 50 lb wire spools for GMA welding (from Stoody Deloro Stellite). For a repair 1/4" deep by 4" wide by 30 ft long (ie 360 cu in), total Stellite required (@.305 lb/cu in) is about 110 lb = $ 5500. Other alloys listed below would all cost no more than $10-12/lb or less. Another problem with Stellite is that it really is not the easiest stuff to deposit crack-free under field welding conditions.

Austenitic Manganese Alloys - McKay makes a MIG welding wire, Tube-Alloy AP-O, which is a work hardening austenitic Mn steel containing about 13% Cr and 16.5% Mn. The Cr should impart very good corrosion resistance. Although deposit hardness is only 18-24 Rc, its high YS of 83,000 psi should resist deformation by the wheel load. It is possible that service will effect the work hardening which can bring hardness up to 50-55 Rc. This alloy should be readily weldable defect-free and relatively easy to grind. Stoody makes a similar wire, Stoody 110-O. There is also a stick (shielded metal arc) Stoody product called Stoody 2110.

Duplex Stainless Steel - Ferralium 255 is a typical duplex stainless steel possessing excellent corrosion resistance (also has about 2% Cu which may resist marine fouling) and very high yield stress (90,000 psi). However, its deposit hardness is not that high, around Rc 20, so it may not be totally suitable. Again available in both stick (McKay 2209 AC-DC) and continuous wire (McKay In-Flux 2209-O).

Build-Up Alloys - Certain alloys are used for building up worn parts and/or for hardfacing to resist further wear. These deposits are quite hard (up to Rc 40) with excellent compression strength and resistance to plastic deformation. Attached examples are Stoody Build-Up and Stoody Super Build-Up GMA wires. However, there is insufficient alloying to impart much more corrosion resistance than found in normal carbon steel.

In summary, none of the above mentioned alloys is perfect for the application in question. Given the choice, I might pick the austenitic

manganese alloys hoping that their initially low as-deposited hardness would be the least significant of the various shortcomings noted, and that work hardening in service would eventually eliminate this.

Certain preparations and precautions should be noted, ie:

- It should be verified that the surface can be adequately cleaned before welding by the proposed technique of sandblasting (ie what is the extent of surface corrosion).

- It is suggested that oxyfuel preheating be used (just ahead of the welding arc) to drive away moisture.

- Welding technique should be assessed beforehand; a minor work program at Research Division could be warranted. Possibly the preferred approach will be to weld from the bottom up (vertical-up) using a full weave.

- The repair is ideally suited for mechanization, but not necessarily to the level of automation of our turbine runner repair robotic system. All steps could probably be performed with a commercially available track/carriage system (with some tailoring to the application) at a substantially higher level of productivity than achievable with manual implementation. These steps would be surface preparation (sand blasting), oxyfuel preheating (mounted on the travel carriage ahead of the welding arc), welding and grinding to a final flat surface. Again, some prior development work at OHRD would be warranted to establish optimum mechanized equipment and techniques.

Mark J. Tinkler
Unit Head - Welding
Metallurgical Research Department

cc W.H.S. Lawson

TECHNICAL DATA
STELLITE 6-O (OPEN ARC)
3/32" DIAMETER

DESCRIPTION

STELLITE 6-O is a continuous, tubular, flux and alloy-cored welding wire for open arc application.

WIRE COMPOSITION

C	1.0 - 1.6	W	3.0 - 6.0
Mn	3.7 Max.	Fe	5.0 Max.
Si	1.0 Max.	Ni	3.5 Max.
Cr	30.0 - 34.0	Co	Balance

Note: The manganese, carbon and iron levels are somewhat higher than in cast STELLITE 6 rods.

WELDING PARAMETERS (DCRP*)

	3/32"
Welding Amperage Range	250 - 500
Welding Voltage Range	24 - 30
Wire Extension	1 - 1 3/4"
Polarity DC Reverse	

DEPOSITION RATE-EFFICIENCY

Size	Amperage	Voltage	Wire Ext.	Lbs./Hr.	Efficiency
3/32"	350	26	1 1/2"	13	85%

The above parameters are in optimum range.

MECHANICAL PROPERTIES

Two layer deposits can be made crack free with proper preheat, interpass temperature and controlled cooling rate.

Hardness HRc	
One Layer	27 - 29
Two Layer	37 - 40

*Base metal dilution DCRP 40-50%.

MAIN LINE

Tube-Alloy® O Flux Cored Open Arc Surfacing Wires

FOR BUILD-UP

McKay Type Open Arc Wires	Description	Dia. & Polarity	Typical Deposit Analysis %	Typical Properties	Wear Properties: Impact Resistance	Wear Properties: Abrasion Resistance	Wear Properties: Weight Loss (Mg) in Abrasive Wear Tests: High Stress	Wear Properties: Weight Loss (Mg) in Abrasive Wear Tests: Low Stress
Tube-Alloy 218-O	Tube-Alloy 218-O deposit is a work hardening austenitic manganese steel alloy. It can be used for build-up or overlay on austenitic manganese steel only. It can also be used for joining austenitic manganese steel to manganese steel. Deposits are extremely tough and work harden rapidly under high impact. Typical Applications: Crusher Rolls • Impact Hammers • Impact Bars • Gyratory Cones • Bucket Teeth • Railroad Frogs • Railroad Crossings	.045 1/16 7/64 DC -	C – 1.0 Mn – 15.0 Si – 0.4 Cr – 3.1 Ni – 0.4 Fe – Bal	Tensile Strength 120,000 psi Yield Strength 80,000 psi Elongation in 2" 32% Hardness – As Deposited 15-22 Rc – Work Hardened 50-55 Rc Machinability Difficult Can be Flame cut	Excellent	Fair	200	730
Tube-Alloy AP-O	Tube-Alloy AP-O deposit is a premium work hardening austenitic manganese steel alloy. It can be used for build-up or overlay on austenitic manganese steel, carbon steel, and low alloy steel. It can also be used for joining austenitic manganese to manganese steel, carbon steel, and low alloy steel. The weld metal has higher toughness than conventional manganese steel weld metal.	1/16 7/64 DC -	C – 0.42 Mn – 18.5 Si – 0.3 Cr – 13.0 Fe – Bal	Tensile Strength 124,000 psi Yield Strength 83,000 psi Elongation in 2" 40% Hardness – As Deposited 18-24 Rc – Work Hardened 50-55 Rc Machinability Difficult Cannot be Flame cut	Excellent	Fair	240	1030
Tube-Alloy BU-O	Tube-Alloy BU-O deposit is a low alloy steel. It is designed for build-up on mild and low alloy steels only. The weld metal has good compressive strength and resistance to plastic deformation, making it an excellent base for surfacing, or a good overlay material where an easily machinable alloy is required. It is not recommended for joining. It should not be stress relieved. Typical Applications: Steel Mill Wobblers • Coupling Boxes • Gear Teeth • Tractor Rails • Tractor Rollers • Mine Car Wheels	.045 1/16 7/64 DC -	C – 0.26 Mn – 0.90 Si – 0.40 Cr – 1.0 Ti – 0.5 Fe – Bal	Hardness – As Deposited, Rc No. of Layers on 1020: 1 – 18; 2 – 22; 3 – 21 No. of Layers on 1045: 1 – 18; 2 – 20; 3 – 21 Can be Flame cut Machinability Excellent	Very Good	Fair	260	1060

FOR OVERLAY

Tube-Alloy 258-O	Tube-Alloy 258-O deposit is a premium martensitic steel alloy. It is a hard, tough H-12 tool steel composition. It is designed only to surface mild and low alloy steel components subject to moderate abrasive wear and/or high temperature (up to 1000F). Proper preheat is required for crack-free deposits. Typical Applications: Machine Components • Dies • Sliding Metal Parts	.045 1/16 7/64 DC -	C – 0.45 Mn – 1.4 Si – 0.8 Cr – 5.0 Mo – 1.5 W – 1.5 Fe – Bal	Hardness – As Deposited, Rc No. of Layers on 1020: 1 – 49; 2 – 53; 3 – 57 No. of Layers on 1045: 1 – 51; 2 – 54; 3 – 57 Can be Flame cut Machinability Grinding Only	Good	Good	150	900
Tube-Alloy 240-O	Tube-Alloy 240-O deposit is a chromium carbide surfacing alloy. It can be used on components subject to severe abrasive wear and heavy impact. The weld metal has higher toughness than conventional chromium carbide alloys due to fewer stress relief check cracks. Typical Applications: • Final Overlays on Roll Crusher Shells • Final Overlays on Hammermill Hammers • Cone Crushers • Shovel Teeth • Augers	.045 1/16 7/64 DC -	C – 3.2 Mn – 1.6 Si – 1.9 Cr – 15.5 Fe – Bal	Hardness – As Deposited, Rc No. of Layers on 1020: 1 – 40; 2 – 48; 3 – 52 No. of Layers on 12-14% Manganese: 1 – 35; 2 – 42; 3 – 50 Cannot be Flame cut Machinability Very Difficult Thickness 3-5 Layers Maximum	Fair	Very Good	175	300
Tube-Alloy 255-O	Tube-Alloy 255-O deposit is a premium high chromium carbide surfacing alloy. It can be used on components subject to extremely severe abrasive wear and moderate impact. It can also be used where high temperature (up to 1750F) wear resistance is required. The weld metal will stress relief check crack. Typical Applications: Similar to those for Tube-Alloy 240-O where additional abrasion resistance is required. Also for: • Cane Pusher Shoes • Muller Tires • Dredging Equipment • Tamping Tines • Fan Blades	1/16 7/64 DC -	C – 4.5 Mn – 0.9 Si – 0.5 Cr – 26.5 Fe – Bal	Hardness – As Deposited, Rc No. of Layers on 1020: 1 – 54; 2 – 58; 3 – 58 No. of Layers on 12-14% Manganese: 1 – 48; 2 – 50; 3 – 53 Cannot be Flame cut Machinability Grinding Only Thickness 2-3 Layers Maximum	Poor	Excellent	130	110

McKAY®

Group 1: Build-Up Alloys

STOODY 110

This is a chromium manganese austenitic stainless steel which is useful for joining manganese steels, also for joining manganese to carbon steels and to some alloy steels.

Stoody 110 has a great affinity for manganese and one of its most common uses is for rebuilding manganese shovel pads and drive lugs. Some railroad companies use it for rebuilding frogs and steel companies for rebuilding wobblers. Stoody 110 offers excellent resistance to cavitation erosion; and it makes an excellent final overlay for applications where impact values are too high for hardfacing (i.e. certain types of crusher hammers). Deposits cannot be flame cut.

SPECIFICATIONS

PRODUCT & PACKAGING	WIRE DIAMETER	TYPICAL WIRE COMPOSITION	SHIELDING	TYPICAL MECHANICAL PROPERTIES	WELDING PARAMETERS Wire Ext.	Amps	Volts
STOODY 110-G 33# Spool	.045"*	Carbon Manganese Silicon Chromium	98% Ar/2% O	Ultimate Tensile Strength: 135 KSI Yield Strength: 101 KSI Elongation in 2": 35.5% Hardness as deposited: 14-20 HRC Work hardened: to 55 HRC	1/2" - 3/4"	160 ± 25	21 ± 3
STOODY 110-O 10# Spool 33# Spool 50# Polypak	.062		Open-arc or CO		1" - 1-1/4"	180 ± 25	24 ± 2

* Can be applied in all positions using 98% argon, 2% oxygen shielding gas.

Welder applying .045" STOODY 110-G to a turbine cone in the overhead position. Welding was done at 190 amperes, 19 volts reverse polarity with a standard C.P. power source. The shielding gas is pure argon. INSET: Close up of a partially rebuilt cavitated area. Deposit thickness in this section was approximately 3". Weldors at this operation preferred .045" STOODY 110-G to other alloys because of its superior all position weldability. Stoody 110-G offers very good resistance to cavitation erosion.

NOTE: Stoody is now licensed (HYDRO-QUEBEC IREQ patented) to produce a new alloy to be known as Stoody Deloro HOI, which offers exceptional resistance to cavitation erosion. A data sheet on this new alloy is available upon request from Stoody at P.O. Box 1901, Industry, CA 91749.

Stainless Steel Weld Metal" was published in the *Welding Journal*, October 1988, pp. 273s-278s. Copies of both are available upon request. A principle conclusion of this work is that, in the as-welded condition, a weld metal ferrite content in the range of 30 to 60 FN, generally assures high strength, high ductility, and high toughness. Above 60FN, ductility and toughness may be unacceptably low. Below 30FN, other studies indicate that corrosion resistance may be unacceptably low.

McKAY 2209 AC-DC (Formerly 2253 AC-DC) COVERED ELECTRODE

One of the latest developments at McKay is the new McKay 2209 AC-DC all-position "Stick" electrode intended for welding one of the most commonly used duplex stainless steels - the "2205" type — where weldments are to be used in the *as welded* condition. Depending upon dilution and specifics of heat treatment, this electrode may or may not be suitable for use in the solution annealed condition.

Available in all standard sizes, McKay 2209 AC-DC duplex stainless steel electrodes operate at the same currents used for standard, austenitic AC-DC stainless electrodes such as E3C8-16. Spatter, slag cover, slag removal, bead configuration and out-of-position welding characteristics are also similar to standard austenitic AC-DC electrodes.

Typical deposit chemistry and properties of undiluted McKay 2209 AC-DC weld metal are shown as follows.

2209 AC-DC

TYPICAL DEPOSIT ANALYSIS (%)	
C	.03
Mn	.95
Si	.45
Cr	23.0
Ni	9.7
Mo	3.0
Cu	–
N	–
Fe	Bal

TYPICAL PROPERTIES	
Tensile Strength	115,000psi
Yield Strength	90,000
Elongation in 2"	27%
CVN Impact @-50F	23 Ft Lbs.
Ferrite	50FN

McKAY IN-FLUX 2209-O (Formerly 2253-O) AND 259-O (Formerly 2553 Cu-O) FLUX CORED OPEN ARC WIRES

Expanding its stainless steel reputation still further McKay has introduced two new grades of duplex stainless steel open arc (self-shielded) flux cored wires for use in "as-welded" applications. McKay In-Flux 2209-O was formulated to complement McKay 2209 AC- DC stick electrodes for welding the "2205" type duplex stainless steels while McKay 259-O was developed for welding Ferralium and CD-4MCu type steels. Again, depending upon dilution and specifics of heat treatment, these wires may or may not be suitable for weldments that are to be solution annealed.

Available in 1/16", 5/64" and 3/32" diameters, these duplex stainless steel wires are operated with the same welding parameters used for standard McKay open arc cored wires such as In-Flux 308L-O or 309L-O and have the same general characteristics as those austenitic grades with respect to low spatter, full slag cover, easy slag removal, bright and finely rippled bead configuration and use in horizontal fillet or flat position applications. Typical deposit analysis and properties of undiluted 2209-O and 259-O weld metal are shown as follows.

TYPICAL DEPOSIT ANALYSIS (%)	2209-O	259-O
C	.02	.02
Mn	1.60	1.0
Si	.40	.30
Cr	22.0	25.0
Ni	8.4	10.2
Mo	3.4	3.0
Cu	–	2.0
N	.14	.14
Fe	Bal	Bal

TYPICAL PROPERTIES	2209-O	259-O
Tensile Strength	116,000psi	122,000psi
Yield Strength	86,000	92,000
Elongation in 2"	30%	28%
CVN Impact @ 50F	85 Ft Lbs.	27 Ft Lbs.
Ferrite	50FN	50FN

In the section on "Filler Metals for Duplex Stainless Steels", caution was urged to avoid excessive dilution. McKay In-Flux, self-shielded duplex stainless wires, having a "softer" arc than prevalent with solid duplex stainless wires in gas metal arc welding, tend to produce less penetration than that experienced with the solid wires. As a result they tend to be more forgiving with respect to adequate ductility in root areas.

Although In-Flux open arc austenitic steel wires like In-Flux 309L are sometimes used with shielding gas such as CO_2 to develop higher ferrite levels in applications where additional crack resistance is required (for example, in overlays on mild steel), In-Flux open arc duplex stainless steel wires should not be used with shielding gas when the deposit is to be used in the as-welded condition. Loss of nitrogen and increase in ferrite would thereby upset the balance of the weld metal composition. However, for use in the post weld heat treated condition, use of shielding gas to increase the ferrite may be acceptable.

WELD METALS TO BE ANNEALED

Filler metal developments for welds that are to be annealed are currently in a state of flux (pun intended). A publication from Teledyne McKay can be expected in the Welding Journal around the end of 1988 or early 1989. Meanwhile, for information on filler metals for annealed weldments of duplex stainless steels, contact Dr. Damien Kotecki at Teledyne McKay.

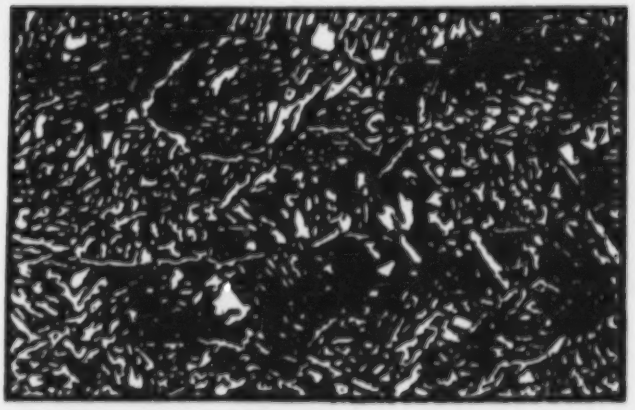

Duplex Weld Metal Microstructure (51FN)
Ferrite is the dark constituent. Kallings Reagent

WELDING PROCEDURE

Under normal conditions, little difficulty is anticipated when welding the duplex stainless steels with McKay filler metals. Most of the 2205 type plate material in use is under 1", with 1/2" and 3/4" sizes predominant. However, the base metal and weld metal are in the high strength range (110,000 to 115,000 psi tensile strength) and hydrogen could be a problem because of the high ferrite content.

Preheating to 200-300F may be necessary in sections over 1/4" and/or where heavily restrained conditions prevail. In all cases, interpass temperatures should be limited to 500F maximum. Dwelling in the 600-1000F range could produce 885F embrittlement. Similarly, dwelling in the 1000-1700F range could produce brittle sigma phase. Hence, beware of exposure in the 600-1700F range.

Excessive dilution into the base metal should be avoided to avert loss of ductility and toughness in the initial layer of weld metal. Refer again to the section on "Filler Metals for Duplex Stainless Steels".

In contrast to procedures for welding many other steels, including austenitic stainlesses, in general for duplex stainless steels, *high* welding heat inputs are preferred, especially if the weldment is to be used in the as-welded condition. High welding heat input is mainly for the benefit of the heat-affected zone. In the heat-affected zone, close to the fusion line, peak temperatures sufficient to cause nearly all of the microstructure to revert to ferrite are reached. High welding heat input results in better heat-affected zone ductility by slowing down the cooling from these peak temperatures and permitting a greater percentage of this "reverted" ferrite to transform back to austenite as the weldment cools.

The information contained herein is based on data developed in the laboratories of Teledyne McKay ("SELLER"), but is presented without guarantee or warranty, and Seller makes no recommendation for, and disclaims any liability incurred from, any use thereof, including without limitation, any use in a commercial process not controlled by Seller and any use in violation of any existing foreign or domestic patent or applicable laws or regulations.

Except as expressly stated in Seller's contract or sales acknowledgement form, all express and implied warranties, including the implied warranties of merchantability and fitness for a particular purpose, are excluded by Seller.

Chemical analyses and properties listed are only typical and are not to be construed as guaranteed values. Tests were performed in accordance with AWS procedures, but individual results may differ depending on conditions of actual use.

TELEDYNE McKAY

Administrative Offices, Research Facilities and Factory:
850 Grantley Road
P.O. Box 1509
York, PA 17405-1509
(717) 848-2490

National Inside Sales Service:
800-34MCKAY (US)
800-356-4300
717-848-2358 Facsimile

TR-62C

Group 1: Build-up Alloys

STOODY BUILD-UP

STOODY BUILD-UP wire contains small percentages of chromium, molybdenum and carbon, as well as manganese, silicon, etc. Hardness is such that deposits have excellent compression strength and resistance to plastic deformation. The product makes an excellent underbase for hardfacing, and is ideal for use on such parts as steel mill wobblers and pods, carbon steel shovel pads, shafting, small rolls, pump parts, etc. Shielding gases which eliminate oxides and nitrides improve both the mechanical properties and the machinability of BUILD-UP deposits.

Just as 7018 mild steel electrodes should not be used as a build up material where high compressive loading is involved, STOODY BUILD-UP wire should not be used for joining. However, elongation of STOODY BUILD-UP-G deposits applied under argon is in the range of 20%.

SPECIFICATIONS

PRODUCT & PACKAGING	WIRE DIAMETER	TYPICAL WIRE COMPOSITION	SHIELDING	TYPICAL ROCKWELL HARDNESS Base Metal	Layers	HRC	WELDING PARAMETERS Wire Ext.	Amps	Volts
STOODY BUILD-UP-G 10# Spool 33# Spool	.045"	Carbon Manganese Silicon Chromium Molybdenum	98% Ar/2% O_2 or 75%Ar/25%CO_2	10% C	2	24-28	1/2" - 3/4"	200 ± 25	21 ± 3
STOODY BUILD-UP-O 10# Spool 33# Spool 50# Polypak	.062"		Open-arc or CO_2	40% C 80% C	2 2	30-35 38-42	1/2" - 3/4"	275 ± 25	26 ± 3

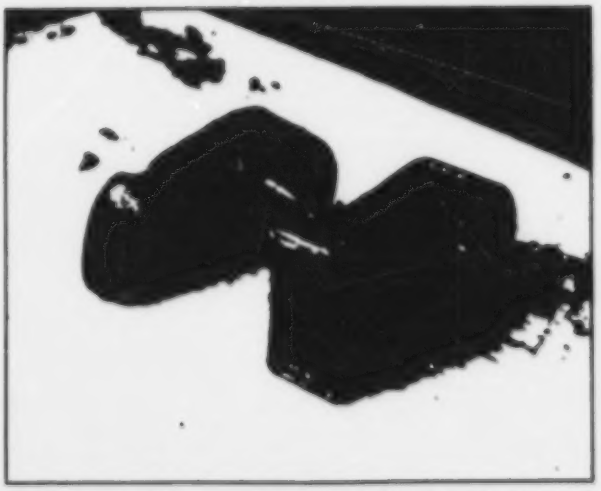

The hammer at left is worn; the one at right was restored to 1/4" of the original size and dimension with 1/16" STOODY BUILD-UP wire, then hardfaced.

Group 2: Moderate Abrasion and Severe Impact

STOODY SUPER BUILD-UP

STOODY SUPER BUILD-UP is a build up material but it is not intended as an underbase for a subsequent layer or layers of another hardfacing alloy. Because of its hardness, wear resistance and mechanical properties, it is used both as the build up and the final overlay.

With normal preheat, STOODY SUPER BUILD-UP can be applied in multiple layers crack free. Deposits of either diameter applied under shielding gases are machinable and will provide excellent service when applied to shafts, undercarriage parts, pump parts, etc.

SPECIFICATIONS

PRODUCT & PACKAGING	WIRE DIAMETER	TYPICAL WIRE COMPOSITION	SHIELDING	TYPICAL ROCKWELL HARDNESS Base Metal	Layers	HRC	WELDING PARAMETERS Wire Ext.	Amps	Volts
SUPER BUILD-UP-G 10# Spool 33# Spool	.045	Carbon Manganese Silicon Chromium Molybdenum	98% Ar/2% O or 75%Ar/25%CO	20° C	2	35-40	1/2" - 3/4"	180 ± 25	21 ± 3
SUPER BUILD-UP-O 10# Spool 33# Spool 50# Polypak	.062"		Open-arc or CO_2	20° C	2	35-40	3/4" - 1"	200 ± 25	24 ± 3

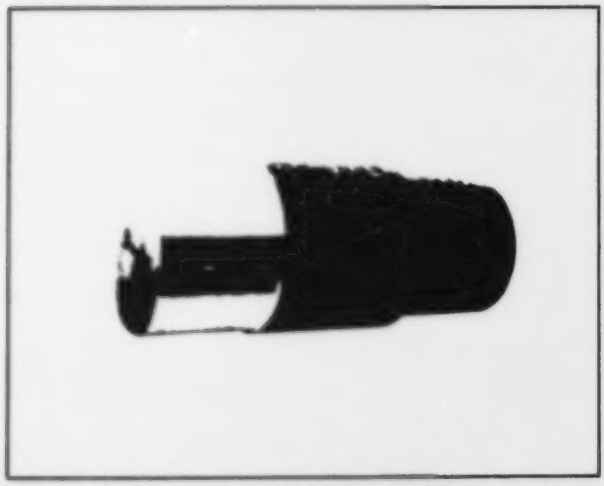

This 2-3/4" OD carbon steel shaft was overlaid automatically with two layers of .045" STOODY SUPER BUILD-UP. Deposit thickness is .425". Welding was done DC Reverse Polarity at 22 volts 190 amperes. Travel speed was 30 IPM and stepover 50% of the previous head.

The shielding gas was 98% argon, 2% oxygen (good results were also obtained with 75% argon, 25% CO_2 although spatter increased slightly).

Machining was done with a Carboloy 888 tool bit. The roughing cut was made at 180 RPM (1696 IPM), .0049" feed; the finishing cut at 450 RPM (4241 IPM), .0049" feed. Hardness reading of the machined deposit was 37 HRC.

People familiar with well drilling know about kelly bars and rolls (which both guide and turn bars during the drilling operation). Here a kelly roll is being hardfaced automatically with 1/16" STOODY SUPER BUILD-UP wire. The user says the application is "working out just fine".

APPENDIX B

ontario hydro

Research Division
800 Kipling Avenue, Toronto, Ontario, Canada M8Z 5S4

August 9, 1990

Mr. Klaus Faisst
Hydraulic Plant Equipment
Hydraulic Generation Operations Division
N10 A1

Abitibi Canyon Headgate Roller Path Repair - Weld Option

1.0 INTRODUCTION

Members of the Applied Mechanics Section were involved briefly in the project. During the meeting on June 26, several methods were proposed for determining forces on the bolts in the restraining plate (see Figure 1). Since the developmental work must be completed very soon, our involvement in the project must be limited as outlined in this memo. Please inform us as soon as possible if you want us to participate in any other work.

2.0 OBJECTIVES

The plate that needs repair will deform during welding. In this memo, a method for constraining these deformations is proposed based on simplified analysis. A more comprehensive work in the aid of the project is outlined.

3.0 RECOMMENDATIONS

A 3/16" plate should be welded at the free end of the repaired plate. The end of the repaired plate at the side plate should be supported by a L3x2x3/8 angle bracket. The new plate and angle bracket should be bolted to the primary concrete every 8.5 inches using 3/4" bolts.

The above conclusions are derived in Section 6 below.

4.0 EXPERIMENTAL STUDY

Due to the time constraints, we may not be able to assist you in the test program currently underway. Forces in the restraining plate could be measured in a laboratory test, if we were given a time period of about six weeks for preparation and testing. However, we would be glad to measure strains (and stresses) in the restraining plate as installed at the station, if you can give us an adequate notice. Should this work be required, please contact Mike Flaman at 405-6998.

Telephone (416) 231-4111 Telex No.: 06-984706 Facsimile (416) 231-9679

5.0 FINITE ELEMENT ANALYSES

Stresses, deformations and forces could be calculated throughout the structure using finite element computer techniques. The analyses could provide optimized bolting configurations and sizing of the new equipment to be installed. Such analysis would take three to four weeks.

6.0 SIMPLIFIED ANALYSIS

A simplified analysis was performed to estimate the size of the restraining plate and bolting requirements. Stresses and deformations in the side plate are also considered. Since deformations in the repaired plate are large, some consideration of plasticity is included.

6.1 Strain in the Repaired Plate

In the initial tests, the largest deformation of 0.433" was measured at the free end. If the plate remained elastic, the force required to restrain this deformation would be:

$$W = 3EIy/l^3 = 114{,}240 \text{ lbs/ft}$$

The smallest radius of deformation would occur at the weld and would equal:

$$R = (d^2y/dx^2)^{-1} = (Mx/EI)^{-1} = 69.5"$$

Strain corresponding to this radius is

$$E = t/2R = 0.010$$

Dr. G. Bellamy tested mechanical properties of the steel plate and found that it has low yield strength of 26.8 ksi /1/ (see Figure 2a). Strain through the plate thickness varies linearly with distance as shown in Figure 2b. Since the strain exceeds elastic limit, stress corresponding to the strain is obtained from the stress-strain curve in Figure 2a (see Figure 2b). The average stress through the plate thickness is about 26,000 psi. Moment (per foot of plate length) producing this stress is:

$$M = S\, t^2\, l\, /\, 4 = 147{,}500 \text{ in-lbs/ft}$$

The force in the retaining plate will be:

$$F = M\, /\, 9.5 = 15{,}500 \text{ lbs/ft}$$

A UNC 3/4 bolt can support a shear force of 11,000 lbs. We recommend that the retaining plate should be mounted with a bolt every 8.5 inches of the plate length. The restraining plate should be 3/16" thick. This would produce a stress of 6,900 psi in the plate.

The repaired plate would not be flat. Considering the effect of the restraining plate, the deformation in the repaired plate would have a shape shown in Figure 3. Because of the plasticity, largest deflection can only be measured experimentally or calculated using finite element method, mentioned above.

The above analysis is conservative because the large deformations at the ends of the repaired plate are not anticipated when the plate is constrained. The weld material will deform plastically as it cools reducing the load carried by the restraining plate and the bolts. This effect can only be determined experimentally.

6.2 Side Plate

The side plate was 39.25" long and 0.375" thick when installed. The plate may buckle due to the deformations in the repaired plate. The largest deformation at the side plate in the unsupported repaired plate is estimated at 0.177". The deformation will occur 8.188" from weld center of the repaired plate. The radius of curvature at the weld is R = 126.3" and the largest strain is E = 0.00545. To pull the tip of the plate to its original position, a bending moment M = S t^2 w/4 = 147,500 in-lbs/ft of plate width will be induced in the weld which will cause plastic strains to occur throughout the section. The force at the side plate that would produce this moment is P = M/l = 18,000 lbs/ft.

A side plate having its original thickness may buckle if the compressive force exceeds a critical force of:

$$Pcr = 2^2 EI/l^2 = 20{,}000 \text{ lbs/ft}$$

From my discussions with Mr. M. Mathers I learned that up to half of the plate thickness may have been lost due to corrosion. For the plate with half thickness, the critical buckling force would be only 2,480 lbs/ft.

If any thickness of the plate is lost due to corrosion, the plate must be reinforced to support the 18,000 lbs/ft load. One option for such reinforcement is to bolt an angle bracket at the top of the side plate before repair. Angle bracket size should be L3x2x3/8. It should be bolted to the primary concrete every 8.5 inches using 3/4 inch bolts. The 3" long edge should be along the side plate and the 2" edge along the repaired plate.

6.3 Effect of Bimetallic Area

In the above calculations, we assumed that bending occurs about the center-plane of the repaired plate. It is not true in the weld area where two metals having different strengths are in contact. Because of the different yield strengths between the two metals and large amount of plasticity, the neutral axis will shift closer to the weld. This will cause further increase in plastic deformation in the parent metal. Stresses in the weld material will be below yield. Tearing may occur between the two metals because of the large plasticity in the parent metal and small elastic deformation in the weld. Cracks may result.

We recommend that a combined experimental and analytical program should be conducted to determine consequences of the proposed weld. Alternatively, weld of mild steel should be used. This should be adequate because the original plate made of low strength steel lasted many years.

Should you require any additional information, please do not hesitate to contact me at 405-6089.

B. Teper
Engineer
Applied Mechanics Section
Mechanical Research Department

DISTRIBUTION

Mr. Mike Markovich	N10-A4
Mr. Ken Matson	N10-A3
Mr. Les Coley	N09-A2
Mr. Kevin Reid	N10-A3
Mr. Mike Martelli	Timmins District
Mr. Gerry Plante	Timmins District
Dr. Scott Lawson	KR 183
Mr. Murray Mathers	KR 072
Mr. Jim Galloway	KR 072
Mr. George Senkiw	KB 214
Mr. Mike Flaman	KB 223
Mr. J.M. Boag	KB 223

REFERENCES

1. Memorandum from G. Bellamy to M. Martelli dated Dec. 19, 1989.

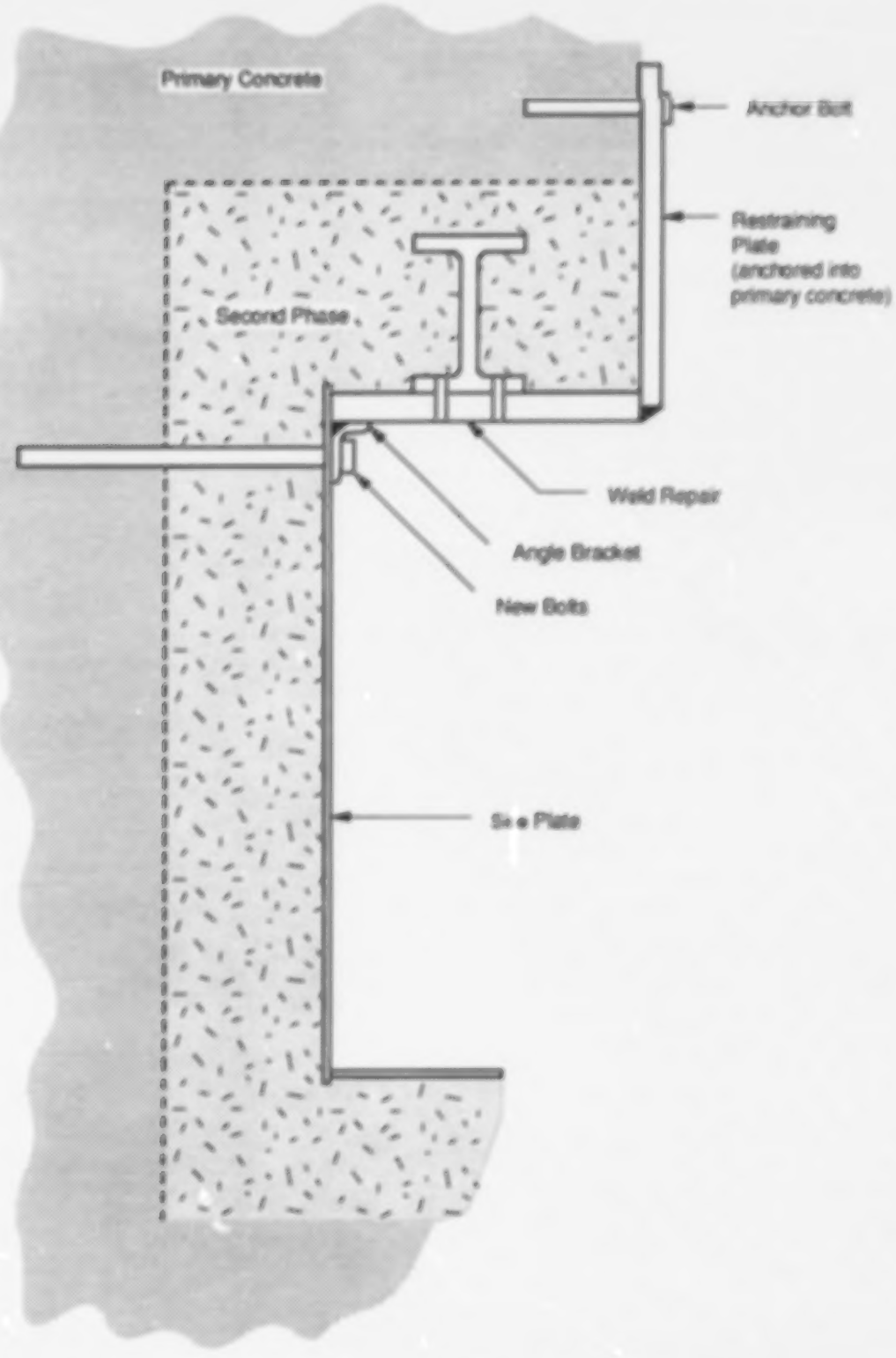

FIGURE 1

PROPOSED SYSTEM OF RESTRAINT

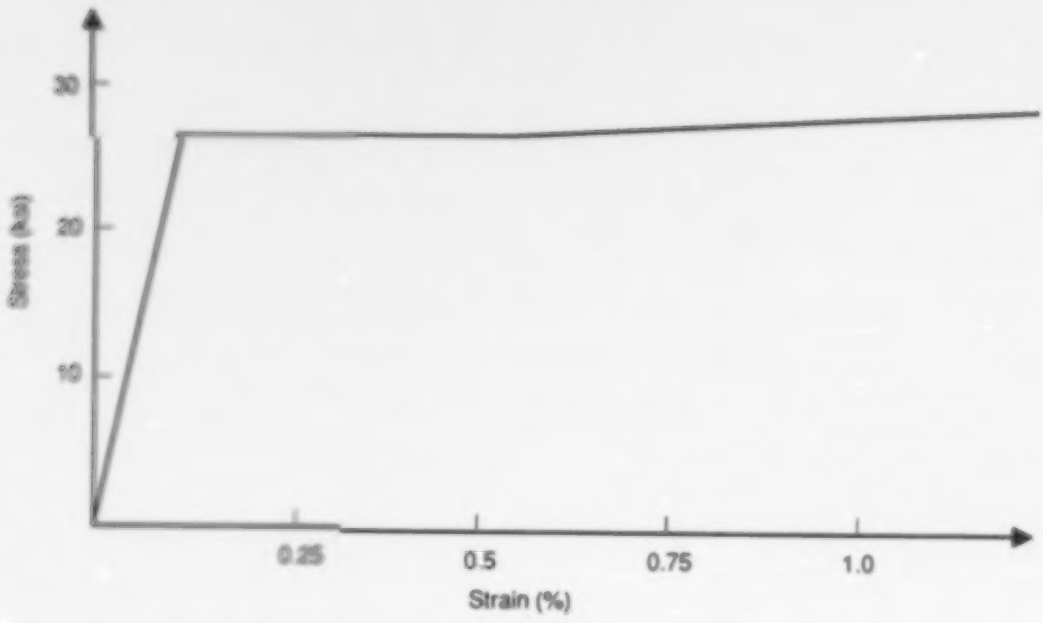

a) Stress-Strain Curve for the Repaired Plate Steel

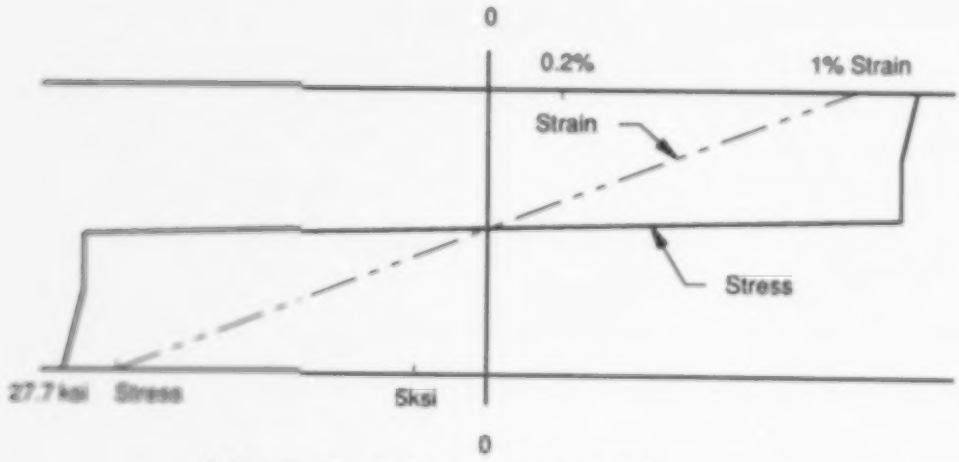

b) StressandStrain Distribution Through Plate Thickness

FIGURE 2

STRESSES IN REPAIRED PLATE

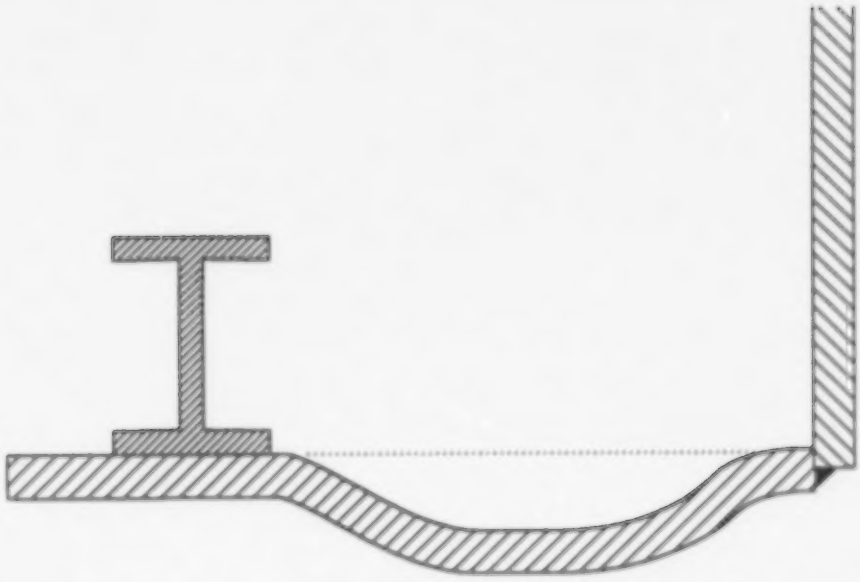

FIGURE 3

DEFORMATION IN REPAIRED PLATE

APPENDIX C

Date: Aug 2,90
Process: Plasma Gouge
Start Location: 6" To 48"
Gouge Time: 2 Min For 8" = 4"/Min 10 Min For 34" = 3.4"/Min

Plasma Pass 1

Time	TC#2	TC#3	TC#4	TC#5	TC#6	TC#7	TC#8	TC#9	TC#10	TC#11	Comments
14:15	51	27		33	46	25	26	29	28	28	Idle
14:16	60	29		34	51	25	52	30	29	28	Start at 6"
14:17	71	33		37	59	27	57	35	30	28	
14:18	71	33		37	90	27	72	35	30	28	Stopped at 14"
14:20	52	46	51	45	111	27	79	42	33	29	Start at 14"
14:22	57	73	87	50	110	28		43	37	31	
14:24	63	88	110	59		32		44	60	34	
14:26	77	101	108	100		38		45	80	67	
14:28	84	106	103	119		59		45	85	100	
14:30	84	104	98	116		103		45	86	104	Stopped at 48"

Date: Aug 2,90
Process: Plasma Gouge
Start Location: 6" To 15" Then 6" To 17" Then 17" To 20.5" Then 20.5 To 48"
Gouge Time : 4 Min For 9" = 2.25 "Min
4 Min For 11" = 2.75 "Min
12.7 Min For 27.5" = 2.16 "Min

Plasma Pass #2

Time	TC#2	TC#3	TC#4	TC#5	TC#6	TC#7	TC#8	TC#9	TC#10	TC#11	Comments
14:41	70	82	78	88	85	83	78	45	78	86	Idle
14:46	68	77	74	81	79	75	72	45	74	80	
14:49	54	70	71	80	79	71	77	45	72	77	Started at 6"
14:50	56	72	72	81	79	70	77	45	72	76	
14:52	82	79	76	86	84	68	82	54	72	75	
14:53	96	87	80	85	83	67	76	58	72	74	Stopped at 15" T 15"
14:56	95	87	83	83	82	65	75	66	73	73	Idle
14:58	80	82	85	84	83	63	81	79	72	71	Started at 6"
14:59	83	83	87	85	83	63	81	82	72	71	
15:00	91	85	90	86	84	61	82	99	73	70	
15:02	96	94	100	88	86	61	78	100	76	70	Stopped at 17"
15:06	100	110	120	86	85	58	77	100	82	69	Idle
15:06:30											Started at 17"
15:07	93	103	116	87	86	57	83	100	83	69	
15:08	96	116	124	90	88	58	86	100	85	69	
15:08:40	103	142	137	93	91	57	83	100	88	69	Stopped at 20.5"
15:12:30	98	130	142	89	87	55	79	99	96	70	Idle
15:13:30	93	118	139	89	87	56	84	96	97	70	Started at 20.5"
15:14:30	93	121	136	90	88	56	84	94	97	70	
15:15:30	94	124	137	92	90	57	85	92	99	71	
15:17:30	98	129	138	103	97	60	89	88	110	79	
15:19:30	111	140	135	148	125	64	103	86	119	101	
15:21:30	122	150	132	190	159	74	112	85	124	123	
15:23:30	121	146	129	179	160	100	113	83	124	159	
15:25:30	120	144	125	173	157	166	123	82	123	156	
15:26:15	120	147	124	170	156	206	134	82	123	153	Stopped at 48"
15:28	120	141	121	164	153	206	144	81	121	148	Cool Down
15:30	117	137	118	155	146	179	138	80	119	142	
15:34	110	128	114	142	135	147	126	78	115	134	
15:40	102	117	108	127	122	123	113	76	109	123	
15:52	91	102	98	109	106		97	72	101	108	

Date: Aug 2,90
Process: Plasma Gouge
Start Location: 6" To 8.5" Then 8.5" To 48"
Gouge Time : .5 Min For 2.5" = 5 "/Min
13.5 Min For 39.5" = 2.9 "/Min

Plasma Pass 3

Time	TC#2	TC#3	TC#4	TC#5	TC#6	TC#7	TC#8	TC#9	TC#10	TC#11	Comments
15:53	78	98	98	111	108	98	104	72	100	108	Started at 6"
15:54:30	102	104	98	109	107	93	98	74	100	106	Stopped at 8.5" at 8.5"
15:56:30	96	100	97	111	108	97	105	80	99	105	Started at 8.5 at 8.5"
15:57:30	96	101	98	110	108	90	105	93	98	103	
15:58:30	99	102	100	110	108	89	104	96	98	103	
16:00:30	107	125	116	115	113	87	109	99	98	102	
16:02:30	114	161	169	121	119	87	113	100	103	102	
16:04:30	118	161	156	132	127	88	116	99	117	106	
16:06:30	136	174	151	202	175	100	132	100	128	132	
16:08:30	133	167	147	189	173	121	130	99	131	166	
16:10	132	164	144	184	171	222	147	98	132	161	Stopped at 48"
16:12	131	160	140	176	166	195	154	97	131	155	Cool Down
16:21	117	137	126	146	141	135	124	92	124	132	
16:25	112	130	119	137	133	124	116	89	120	126	

Date: Aug 2,90
Process: Plasma Gouge
Start Location: 21" To 33"
Gouge Time : 5 Min For 12" = 2.4 "/Min

Plasma Pass 4

Time	TC#2	TC#3	TC#4	TC#5	TC#6	TC#7	TC#8	TC#9	TC#10	TC#11	Comments
16:28:30	106	121	113	134	131	117	110	86	118	122	Started at 21"
16:29:30	107	126	114	136	133	115	109	86	117	120	
16:30:30	111	138	118	140	136	115	109	85	119	120	
16:31:30	114	146	122	147	140	115	109	84	124	121	
16:32:30	119	152	124	160	147	115	109	84	131	122	
16:33:30	126	159	125	192	163	117	109	83	136	126	Stopped at 33"
16:39	121	149	122	172	161	106	104	81	140	147	Cool Down
16:55	101	119	110	126	123	93	92	77	123	124	-
17:06	93	107	107	103	112	80	85	73	112	114	-
17:22	84	97	96	98	98	77	80	70	103	102	-
17:42	74	82	85	84	84	70	73	65	92	90	-
18:04	67	73	77	75	75	63	69	63	82	81	-
18:23	63	69	72	69	70	59	65	61	76	75	-

Date: Aug 2,90
Process: Welding
Start Location: 34.25" To 29.25", 29.25" To 20.25
Weld Time : 13 Min For 5" = 0.385 "/Min
19 Min For 9" = 0.474 "/Min

Weld Pass #1

Time	TC#2	TC#3	TC#4	TC#5	TC#6	TC#7	TC#8	TC#9	TC#10	TC#11	Comments
18:23:45	63	69	71	84	80	59	61	61	75	76	Started at 34.25"
18:26:45	79	85	71	129	108	58	72	60	75	97	
18:28:45	87	93	70	162	130	58	80	60	85	121	
18:30:45	91	99	70	171	146	58	83	60	75	138	
18:32:45	94	97	70	174	146	58	83	60	74	147	
18:34:45	95	100	70	164	148	58	82	59	75	151	
18:36:45	90	96	70	158	143	58	92	59	76	150	Stopped at 29.25"
18:38	92	98	70	156	141	59	78	59	77	150	Started at 29.25"
18:40:30	90	98	70	145	135	60	77	59	80	146	
18:42	90	98	71	141	132	60	76	59	82	143	
18:44	91	100	72	137	130	60	76	58	86	140	
18:46	91	101	73	133	127	61	74	58	94	137	
18:48	91	104	76	130	125	62	73	58	100	135	
18:52	93	116	87	125	120	63	74	60	118	131	
18:54	95	123	103	124	121	64	74	61	130	128	
18:56	99	143	114	124	121	63	77	61	141	126	
18:57	99	143	114	124	121	63	77	61	141	126	Stopped at 20.25"
19:02	88	134	130	124	121	64	91	60	154	121	Cool Down
19:05	86	125	124	119	116	64	89	60	142	119	"
19:37	73	87	91	94	91	63	76	58	102	101	"
19:43	70	83	86	89	87	62	74	58	98	96	"

Date: Aug 3,90
Process: Welding
Start Location: 20" To 15.5"
Welding Time: 9.5 Min For 4.5" = 0.474 "/Min

Weld Pass #1a

Time	TC#2	TC#3	TC#4	TC#5	TC#6	TC#7	TC#8	TC#9	TC#10	TC#11	Comments
19:55:45	75	90	80	76	76	60	53	57	91	88	Started at 20.25"
19:57:45	81	115	87	80	80	60	59	57	90	87	
19:59:45	88	149	113	86	86	60	65	56	93	86	
20:01:45	92	168	132	89	89	59	69	51	97	85	
20:03:45	94	476	135	88	88	59	60	57	102	84	
20:05:15	94	476	135	88	88	59	60	57	102	84	Stopped at 15.5"
20:12	75	117	137	84	84	57	76	59	105	81	Cool Down
20:21	70	96	108	79	79	56	71	58	102	79	"
20:41	65	77	88	73	73	54	65	58	91	75	"

Date: Aug 3,90
Process: Welding
Start Location: 48" To 46", 46" To 43", 43" To 36", 36" To 35.75", 35.75" To 23.5", 23.5 To 16.75, 16.75" To 6"

Weld Time :
6.5 Min For 2" = .308"/Min
8.5 Min For 3" = .353"/Min
20.75 Min For 7" = .337"/Min
1 Min For .75" = .250"/Min
25.5 Min For 12.25" = .480"/Min
20 Min For 6.75" = .338"/Min
32.5 Min For 10.75" = .331"/Min

Weld Pass #2

Time	TC#2	TC#3	TC#4	TC#5	TC#6	TC#7	TC#8	TC#9	TC#10	TC#11	Comments
18:18	31	33	33	33	33	29	31	32	35	34	Idle
8:44	30	33	32	33	32	29	30	32	34	33	Started at 48"
8:46	38	40	32	41	40	207	65	32	34	33	
8:48	39	41	32	43	43	250	83	31	34	33	
8:50	45	47	32	49	48	242	95	31	34	34	
8:50:30	45	47	32	49	48	242	95	31	34	34	Stopped at 46"
9:00	40	41	32	45	43	112	65	31	34	36	Started at 46"
9:02	42	44	32	48	46	153	70	31	34	37	
9:04	42	45	32	49	48	174	83	31	34	38	
9:06	44	46	32	51	50	184	91	31	34	39	
9:08	46	49	32	54	52	188	90	31	34	41	
9:08:30	47	49	32	54	52	188	92	31	34	41	Stopped at 43"
9:17:45	46	48	32	58	57	142	83	31	34	51	Started at 43"
9:19:45	46	48	32	59	57	133	80	31	34	53	
9:21:45	47	49	32	62	58	134	77	31	35	54	
9:23	48	50	32	63	59	136	78	31	35	55	
9:25	48	51	33	64	62	138	80	31	35	58	
9:27	50	53	33	68	66	141	82	31	35	63	
9:29	53	55	33	75	70	141	83	31	35	70	
9:31	55	58	33	81	76	141	84	31	35	80	
9:33	58	61	33	89	87	140	87	31	36	95	
9:35	62	65	34	102	99	139	92	31	36	110	
9:37	68	71	34	124	110	138	95	31	36	127	
9:38:30	77	76	34	139	124	136	109	31	37	150	Stopped at 36"
10:18	53	58	42	75	74	88	74	31	47	87	Idle
10:23	51	57	42	76	75	83	64	31	48	83	Started at 36"
10:24	56	62	42	90	82	82	66	31	48	88	Stopped at 35.75"
10:24:30	57	63	42	98	86	82	69	31	48	91	Started at 35.75"
10:26:30	66	72	42	127	113	80	77	31	48	107	
10:28:30	76	83	42	172	146	79	87	31	48	139	
10:30:30	85	91	43	202	170	78	92	31	49	170	
10:32:30	88	95	43	210	184	77	96	31	48	182	
10:34:30	89	96	43	207	180	76	94	32	49	188	
10:36:30	89	96	43	200	174	76	91	31	50	189	
10:38:30	88	94	44	186	174	76	90	31	51	187	

Date: Aug 3,90
Process: Welding
Start Location: 48" To 46", 46" To 43", 43" To 36", 36" To 35.75", 35.75" To 23.5", 23.5 To 16.75, 16.75" To 6"

Weld Time :
6.5 Min For 2" = .308"/Min
8.5 Min For 3" = .353"/Min
20.75 Min For 7" = .337"/Min
1 Min For .75" = .250"/Min
25.5 Min For 12.25" = .480"/Min
20 Min For 6.75" = .338"/Min
32.5 Min For 10.75" = .331"/Min

Weld Pass #2 - Continued

Time	TC#2	TC#3	TC#4	TC#5	TC#6	TC#7	TC#8	TC#9	TC#10	TC#11	Comments
10:40:30	86	94	44	182	166	76	88	32	52	184	
10:42:30	85	94	45	175	159	76	86	32	55	179	
10:44:30	84	93	45	166	157	77	86	32	58	174	
10:46:30	84	94	46	161	153	77	86	32	62	170	
10:48:30	84	96	48	156	147	77	84	32	68	165	
10:50:30	83	95	50	151	144	78	83	32	75	161	
10:52:30	84	97	53	146	140	78	82	32	86	156	
10:54:30	83	100	57	143	138	78	83	32	44	153	
10:56:30	84	105	62	140	134	76	82	32	102	149	
10:58:30	85	108	67	138	132	78	82	33	108	146	
11:00	85	105	74	138	134	78	95	33	120	143	Stopped at 23.5"
11:05	86	122	91	130	126	77	81	33	127	137	Started at 23.5"
11:07	86	123	97	128	125	77	81	35	128	136	
11:09	89	135	103	127	124	77	81	33	133	133	
11:11	91	154	119	127	123	77	83	34	142	131	
11:13	96	168	131	128	126	77	87	34	148	129	
11:15	99	195	147	131	129	76	104	34	153	127	
11:17	102	216	167	130	127	76	91	35	155	125	
11:19	103	130	190	128	126	76	90	35	154	123	
11:21	105	224	193	128	126	75	89	35	153	121	
11:23	104	215	195	126	124	75	90	36	152	119	
11:25	105	207	192	123	122	75	90	36	152	118	Stopped at 16.75"
11:48	80	115	118	103	103	70	86	45	123	104	Idle
12:32	66	78	85	78	79	61	69	51	92	84	Idle
12:33:45	77	86	83	74	74	61	55	51	91	83	Started at 16.75"
12:35:45	80	92	86	73	73	60	54	51	90	83	
12:37:45	82	99	94	74	74	60	54	51	89	81	
12:39:45	83	102	100	75	75	59	57	51	88	81	
12:41:45	86	108	106	74	74	59	56	52	88	81	
12:43:45	89	108	109	75	75	59	58	52	88	79	
12:45:45	89	109	109	75	75	58	58	53	88	79	
12:47:45	93	111	109	75	75	58	56	54	89	78	
12:49:45	98	110	109	75	75	58	59	55	89	78	
12:51:45	100	111	109	75	75	58	58	57	89	77	

Date: Aug 3.90
Process: Welding
Start Location: 48" To 46", 46" To 43", 43" To 36", 36" To 35.75", 35.75" To 23.5", 23.5 To 16.75, 16.75" To 6"

Weld Time : 6.5 Min For 2" = .308"/Mn
8.5 Min For 3" = .353"/Mn
20.75 Min For 7" = .337"/Mn
1 Min For .75" = .250"/Mn
25.5 Min For 12.25" = .480"/Mn
20 Min For 6.75" = .338"/Mn
32.5 Min For 10.75" = .331"/Mn

Weld Pass #2 - Continued

Time	TC#2	TC#3	TC#4	TC#5	TC#6	TC#7	TC#8	TC#9	TC#10	TC#11	Comments
12:53:45	107	113	10	76	76	57	58	61	90	76	
12:55:45	113	112	108	77	77	57	61	102	87	76	
12:57:45	120	112	107	76	76	57	58	101	88	76	
12:59:45	134	116	107	80	80	56	64	101	88	75	
13:01:45	160	118	107	83	83	56	67	99	92	74	
13:03:45	182	122	107	88	88	56	71	99	91	74	
13:05:45	210	122	106	88	88	55	91	99	91	74	
13:06:15	210	122	106	88	88	55	91	99	91	74	Stopped at 6"
13:18	124	104	108	86	86	54	79	100	90	72	Cool Down
13:50	88	83	92	73	73	50	67	87	90	67	"
14:09	93	81	83	63	63	49	52	8[illegible]	79	65	"

90-137
184578-026-RD

APPENDIX D

TABLE D1

LOADS DURING FIRST PLASMA PASS

Time	Load Cell Loads (Klb)			
	1	2	3	Total
14:15	0.00	0.00	0.00	0.00
14:16	-1.07	-0.57	-0.58	-2.22
14:17	-2.31	-1.07	-0.25	-3.62
14:20	-0.91	-1.07	-0.41	-2.38
14:24	2.89	-0.74	-0.90	1.24
14:30	7.59	1.56	1.15	10.30

TABLE D2

LOADS DURING FINAL PLASMA PASS

Time	Load Cell Loads (K.lb)			
	1	2	3	Total
14:41	8.33	3.93	12.25	24.51
14:49	7.83	4.43	11.26	23.52
14:52	4.37	3.52	11.35	19.24
14:56	7.09	3.61	11.26	21.96
15:00	10.89	4.75	11.18	26.82
15:06	11.55	4.10	11.10	26.74
15:08:40	11.63	4.10	11.02	26.74
15:12:30	13.52	4.51	11.76	29.79
15:15:30	14.84	5.82	12.09	32.75
15:17:30	13.52	4.43	11.26	29.21
15:19:30	15.01	5.25	12.00	32.26
15:23:30	16.99	7.87	13.40	38.26
15:25:30	17.57	7.95	15.37	40.89
15:28	18.06	8.77	20.06	46.89
15:34	17.24	9.92	23.68	50.83
15:40	16.74	10.25	22.36	49.35
15:52	16.58	10.66	21.21	48.44
15:53	16.58	10.66	21.21	48.44
15:54:30	14.68	10.16	21.46	46.30
15:56:30	13.19	9.84	21.29	44.32
16:00:30	13.19	9.84	21.29	44.32
16:02:30	16.58	9.43	21.05	47.05
16:04:30	21.28	10.74	21.21	53.22
16:06:30	23.09	12.54	22.11	57.75
16:08:30	23.91	14.10	24.09	62.10
16:10	24.08	15.08	28.69	67.85
16:12	23.83	15.49	30.01	69.33
16:21	23.17	15.98	29.43	68.59
16:25	22.84	16.07	28.69	67.60
16:30:30	22.60	16.15	28.03	66.78
16:31:30	21.11	13.61	26.97	61.68
16:33:30	22.10	13.03	26.80	61.93
16:39	23.83	16.72	30.01	70.56
17:22	22.76	17.79	27.46	68.01
18:23	22.35	17.21	25.40	64.97

TABLE D3

LOADS DURING FIRST WELD PASS

Time	Load Cell Loads (K.lb)			
	1	2	3	Total
18:26:45	22.35	17.20	25.40	64.96
18:30:45	22.43	17.04	26.39	65.86
18:34:45	23.01	18.43	28.69	70.13
18:40:30	22.93	19.33	30.66	72.92
18:46	24.24	19.25	31.32	74.82
18:52	24.90	19.91	32.14	76.96
18:56	25.65	20.40	32.56	78.60
19:02	26.72	21.46	32.97	81.15
19:05	26.39	21.06	32.72	80.16
19:37	24.99	20.73	30.75	76.46
19:43	24.99	20.73	30.58	76.30
19:55:45	24.12	19.76	30.09	73.97
19:59:45	24.00	19.26	30.34	73.60
20:03:45	25.98	21.39	30.91	78.28
20:05:15	27.96	22.62	31.40	81.98
20:12	27.46	22.05	31.40	80.92
20:21	27.21	21.97	31.16	80.34
20:41	26.55	22.05	30.83	79.43

TABLE D4

LOADS DURING FINAL WELD PASS

Time	Load Cell Loads (K.lb)			
	1	2	3	Total
8:44	26.64	19.51	30.01	76.15
8:48	26.76	19.14	30.71	76.61
8:50:30	26.76	19.14	30.71	76.61
9:00	26.31	20.25	31.90	78.45
9:02	26.59	19.92	32.68	79.19
9:04	26.55	19.76	35.27	81.58
9:08:30	26.27	21.64	35.76	83.67
9:17:45	26.18	21.52	33.30	81.00
9:21:45	26.27	21.31	35.60	83.18
9:27	26.31	22.13	37.61	86.05
9:33	26.51	23.08	39.46	89.05
9:37	26.64	23.36	36.09	86.09
9:38:30	26.72	23.81	41.72	92.25
10:18	25.73	24.06	39.46	89.25
10:23	25.69	23.48	38.52	87.69
10:28:30	25.89	22.83	39.13	87.86
10:32:30	26.31	23.77	41.64	91.72
10:38:30	26.80	24.43	43.04	94.27
10:42:30	27.21	25.00	43.65	95.87
10:48:30	27.54	25.33	44.15	97.02
10:54:30	27.96	25.82	45.09	98.87
10:58:30	28.45	26.15	44.72	99.32
11:00	29.60	27.26	44.97	101.83
11:05	29.03	26.35	44.44	99.82
11:09	28.49	25.41	44.48	98.38
11:13	29.60	27.46	44.97	102.03
11:17	30.68	28.36	45.22	104.26
11:23	31.25	28.85	45.22	105.32
11:25	32.33	29.10	45.22	106.64
11:48	30.84	29.43	43.98	104.25
12:32	30.59	30.17	43.24	104.00
12:33:45	29.85	29.35	43.24	102.44
12:37:45	28.70	29.18	43.49	101.37
12:43:45	31.01	30.41	43.65	105.07
12:47:45	33.98	30.99	43.74	108.70
12:53:45	36.45	31.48	43.41	111.33
12:57:45	38.51	31.89	43.16	113.56
13:03:45	39.83	32.13	42.91	114.88
13:06:15	41.97	32.54	42.42	116.94
13:18	43.05	32.54	41.68	117.27
13:50	43.46	33.12	40.86	117.43
14:09	43.46	33.12	40.86	117.43